Lithium Combustion: An Update

Martin Schiemann*[1], Jeffrey Bergthorson[2], Peter Fischer[1, 3], Viktor Scherer[1], Dan Taroata[3], Günther Schmid[3]

[1] Department of energy plant technology, Ruhr-University, Bochum, Germany

*+49 234 32 27362; schiemann@leat.rub.de

[2] Department of Mechanical Engineering, McGill University, Montreal, QC, Canada

[3] Siemens AG, Corporate Technology

Abstract – The combustion of lithium has been subject of research for several decades. The focus has been put on safety issues, such as lithium spill fires from spills in nuclear reactors, or as a propellant in the atmosphere of foreign planets. While the former was typically investigated by combustion in pool fires and molten pieces of lithium, the latter was also investigated in experiments with packed beds of lithium particles. The current work is triggered by a new approach to use lithium as an energy carrier in a closed energy loop based on lithium combustion, followed by a subsequent reduction of the solid-phase combustion products via electrolysis to elemental lithium again.

This paper summarizes the existing knowledge on lithium combustion. It presents the available findings on lithium combustion for large single pieces of lithium, on pool fires, reaction in packed beds as well as the combustion of sub-mm sized particles and droplets which are needed for the novel process design mentioned above. The combustion reactions of lithium with N_2, O_2, H_2O and CO_2 are discussed. Numerical modelling of lithium particle combustion is a new field in lithium combustion research. It is discussed to show its potential for future combustion characterization.

Keywords: Lithium, combustion, energy storage, renewable energy, metal fuel

1 Introduction

Lithium combustion with different gaseous species has been of interest for several reasons in the past. In fusion reactors, lithium is used as a tritium breeder blanket and as coolant [1–3]. As lithium spills are known to be extremely hazardous [4], research on lithium fires has been carried out to understand the combustion process

and to improve the extinguishing procedure of such fires [5]. Another application, which induced research on the combustion of lithium, is the utilization of Lithium as a propellant for torpedoes [5,6] or rockets [7,8].

The increasing demand for environmentally friendly energy provision, mainly the reduction of greenhouse gas emissions [9], has led to a growth in renewable energy from solar or wind power. As the temporal availability of these energy sources does not necessarily coincide with the demand for energy, large scale storage techniques are needed. As will be shown, lithium is capable to act as storage material in combination with a combustion process.

Metals have been considered as a mechanism for storing energy for some time, due to their high energy densities and specific energies [10–18]. Indeed, the high energy content in metals has long motivated their use as energetic additives in energetic materials, slurry fuels and propellants [19–29]. In order to harness the chemical energy in the metal fuels, most previous studies have considered the reaction of various metals, specifically aluminum and magnesium, with water to produce hydrogen on demand [10,11,13–15,17,30,31], with only a small number of studies considering the combustion of the metal fuels to produce heat [12,16,32–34].

Lithium has a very low electronegativity (0.98 on the Pauling scale). It is situated closely to hydrogen on the periodic table of the elements, with an atomic number of 3 and atomic weight of 7 a.m.u., such that it has a high amount of chemical energy, in its available valence electron, compared to its mass – leading to its high specific energy. Indeed, lithium has the third highest specific energy (kJ/kg) of all metals/metalloids, behind only boron and beryllium [34]. The high specific energy of lithium motivates its use as the anode material within lithium-ion, as well as lithium-oxygen or lithium-air, batteries [35–37]. Lithium has been proposed as an energy carrier, or energy-carrying component, within systems that would generate hydrogen using the lithium-water reaction, or lithium hydrides and borohydrides [38–41]. It has also been used as a chemical fuel for underwater propulsion systems [42–44].

Like all electro-positive metals, lithium shows properties which make it a promising candidate to act as storage material in energy circuits based on renewable energy [16,45,46]. Its ability to react exothermally with typical components in fossil-fuel fired power plant exhaust gases (beneath CO_2, H_2O, O_2, Lithium even reacts with N_2) leads to the idea to build a thermal process, in which an exhaust gas mixture (from conventional fossil fuel fired power plants) or a pure gas stream (which could be CO_2 or N_2, both being produced in CCS power plants [47]) is used to react with lithium. Figure 1 shows a schematic flow sheet of a process, in which the energy production

cycle based on lithium is closed, as the combustion products lithium carbonate, lithium nitride or lithium oxide are converted to lithium by renewable energy, therefore lithium acts as storage material for renewable energy here. It has favourable properties compared to other storage materials, e.g. high density (Li and reaction products are solid at ambient conditions) and high ability to be regenerated by electrolysis.

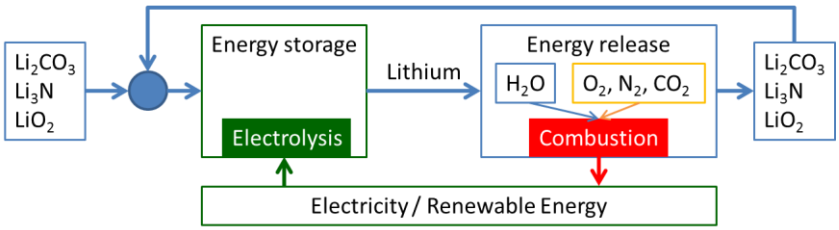

Figure 1: Process flow sheet of lithium-based energy storage and production cycles

The reaction of lithium with different exhaust gas components lead to different by-products (e.g. CO or H_2), which are valuable materials for chemical processes and optimize the economic balance of the process. The economical boundaries for a lithium based process can be roughly estimated from current market prices for lithium compounds. A power plant producing 100 MW_{th} or 35 MW_{el} requires 9.3 t_{Li}/h using CO_2 as gaseous reaction partner. The produced amount of Li_2CO_3 is 50 t/h, which has to be recycled by electrolysis. In 2012, the global market price for Li_2CO_3 was approx. 6000 $/t [48]. Assuming a lithium loss of 1% in the process circuit means costs of 0.83 $/$kWh_{el}$, which is high for current electricity prices. Several factors have to be considered for an economical calculation, e.g the value of the products like CO and Li_2CO_3 and the potential use of pure lithium or Li_2O as refill, changing the cost structure of the process. Furthermore, sodium is known to show similar combustion phenomena, and the investigation of lithium combustion is a good pilot process to investigate the combustion of metals as chemical energy storage materials.

The current status of literature available cannot provide enough information for a sound process design. Controlled combustion requires stable flames and sufficient burn-out, which makes the process economically feasible. Typical processes, which are well established and could be examples for such a process, are pulverized coal and liquid fuel combustion. In both processes, droplets or particles in a size range 10 - 100 µm are burned, leading to stable flames due to good ignition and sufficient burn-out. Finally, an effective technique to recover the combustion residues, ash-like lithium compounds, is needed for complete recycling of lithium. As techniques

are available [49] to electrolyse lithium from different lithium salts like lithium carbonate [50] or lithium chloride [51], this step is not discussed in detail here.

The current work addresses several aspects of lithium combustion. First, general chemistry and thermodynamic data available and necessary for calculations of the combustion process are discussed. In the following combustion experiments of lithium with different gaseous species are described, starting with large scale pool or block samples. A section on the combustion of single particles and first experiments with lithium spray combustion, including a short section on modelling of lithium particle combustion closes the discussion on literature. From the summarized knowledge question arise, which are presented in the conclusion.

2 Combustion of Lithium

2.1 Phenomenology of Lithium Combustion

The combustion of metals is a complex process affected by many sub-processes, including evaporation, gas phase reactions and aerosol formation. The reaction products condense at high temperatures and even solidify at temperatures of several hundred Kelvin. Reviews on the combustion properties of lithium have been presented before by Jeppson [1] and Rhein [52]. Both focused on combustion of pools, blocks and packed beds. They already summarize important data, which is very helpful to understand general effects during lithium combustion. The combustion of single particles, droplets or sprays is relatively new and offers new aspects to the lithium combustion knowledge base.

2.2 Reactions, Reaction Enthalpies

Table 1: Exothermal reactions of Li with exhaust gas components calculated with data from [53], #7: [kJ/mol$_C$].

Reaction #	Chemical reaction	Reaction enthalpy [kJ/mol$_{Li}$] (298.15 K, 0.1 MPa)
1	$6\ Li + N_2 \rightarrow 2\ Li_3N$	-54
2	$2\ Li + 2\ CO_2 \rightarrow Li_2CO_3 + CO$	-270
3	$2\ Li + 1\ CO_2 \rightarrow Li_2O + CO$	-157
4	$4\ Li + 1\ CO_2 \rightarrow 2\ Li_2O + C$	-201
5	$2\ Li + 2\ H_2O \rightarrow 2\ LiOH + H_2$	-202
6	$4\ Li + O_2 \rightarrow 2\ Li_2O$	-299
7	$C + O_2 \rightarrow CO_2$	-394

Different Lithium gas reactions are available to design exothermal processes. Table 1 summarizes the reactions of lithium with the major power plant exhaust gas constituents, considering educts, products and reaction enthalpies per mole lithium. The carbon oxidation reaction is given for comparison. Except the reaction of lithium with nitrogen, all reactions provide at least 40% of the molar enthalpy released from carbon oxidation, which makes them possible candidates for energy processes. Furthermore the specific energy is higher than for typical liquid hydrocarbon fuels (gasoline, diesel) [34], coal or biomass, and the ability to produce CO from CO_2 offers new ways of energy production.

2.2.1 Aggregate states

The different reaction products, LiOH, Li_2CO_3 and Li_2O change their aggregate states at very different temperatures, which makes a defined process control complicated. Furthermore, the thermal stability is limited and different compounds tend to decompose at temperatures relevant for combustion processes. Figure 2 summarizes the aggregate states depending on temperature of the important lithium compounds according to [53].

Lithium melts at 453 K [1,53–55], although slight deviations ranging from 452 K to 459 K are known in literature [56–58]. The boiling point is 1620 K according to [53], while values up to 1643 K are reported [57,58].

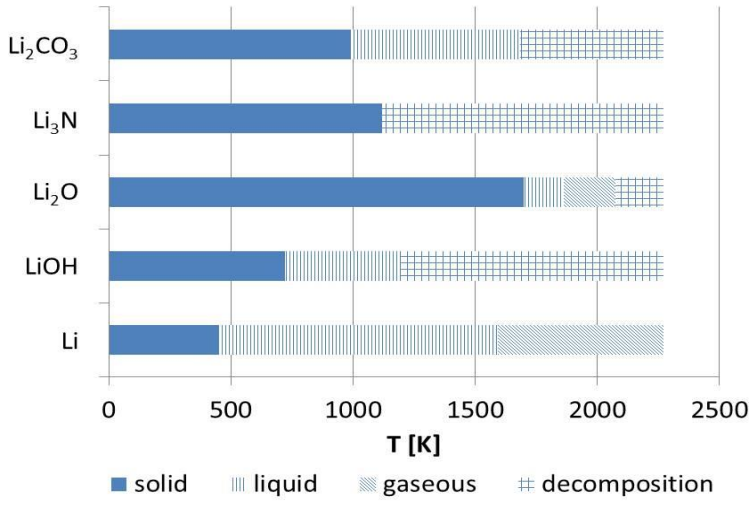

Figure 2: Summary of aggregate states according to [53].

Due to the high molar reaction enthalpy, reactions 2 and 6 in Table 1 appear as most promising in respect to energy processes. The fusion temperature of Li_2CO_3 is 993 K, as reported in [59]. In the same work, Reisman also

mentions two transitions in the crystal lattice at 523 K and 683 K, for which the enthalpies are also stated in [59]. Instead of a boiling point, Li_2CO_3 is reported to decompose at temperatures above 1583 K [60–62]. Timoshevskii et al., who investigated the thermal decomposition of Li_2CO_3 melts achieving the efficient production of Li_2O, mention the hindered decomposition by elevated partial pressures of CO_2 [62]. In fact, at the melting point of Li_2CO_3 the saturation pressure of CO_2 above the sample surface is 533 Pa, which prevents the carbonate from further decomposition. Furthermore it is reported, that at temperatures above 1643 K, the saturation pressure reaches 10^5 Pa, so that further temperature increase under atmospheric pressure should lead to complete decomposition in short time scales [61].

Li_2O has the highest fusion temperature of all lithium compounds considered. Nevertheless, the exact value is not completely certain, as Brewer et al. report a value of 1900 K [63], while van Arkel et al. measured 1843 K as melting temperature [64], and Ortman and Larsen published 1700 K [65]. With increasing temperature, the decomposition of Li_2O increases producing gaseous LiO, Li_2O_2, O_2 and pure Li beneath Li_2O [66–68].

Li_3N melts at 1088 K [69], as Yonco et al. measured at a nitrogen pressure of $1.6 \cdot 10^5$ Pa. No melting point at atmospheric pressure has been reported, as the decomposition process starts around 973 K. Above this temperature, an increase of nitrogen pressure in an enclosed system, in which the Li_3N was heated under inert conditions, was measured, indicating severe decomposition [69]. As is shown in section 2.2.3, a temperature of 1234 K is also known and used in different thermodynamics codes. Ref. [53] does not list a decomposition temperature at all.

The melting point of LiOH was found to be 746 K [70,71]. Kudo reports, that even in the solid phase below 713 K decomposition takes place [72], which is also reported by Dinh et al. [73]. A boiling point has been reported at T_{vap}= 1899 K, determined as the temperature at which the fugacity of LiOH becomes 1 atm for the process LiOH(l)=LiOH(g) [53]. In experiments where Li reacted with water vapour, a limiting temperature of 473 K was reported for the reaction $2Li + 2H_2O \rightarrow 2LiOH + H_2$, above only Li_2O was found to be the reaction product [52]. According to the phase change data, reaction 5 in Table 1 is very unsuitable to reach high process temperatures when LiOH is achieved as final product.

2.2.2 Heat Capacities

Just as the phase change temperatures are varying for the different compounds, the heat capacities span a certain range as is shown in Figure 3, which is based on the summarized data from [53]. The molar heat capacity of Lithium is low compared to the reaction products, it ranges from 24.7 J/(mol*K) (solid, 300 K) to 30.3 J/(mol*K) (solid, 453 K). Douglas et al. present relevant data in the temperature range from 289 K to 1173 K [54]. Novikov et al. have similar data [74], but their values are approx. 10% lower. In [53] it is mentioned that for higher temperatures, the data were extrapolated in a "reasonable manner", which is not described in detail. Vargaftik et al. [75] list equal values for temperatures up to the boiling point, but provide additional data for the heat capacity of lithium vapour between 40.16 J/(mol*K) (1700 K) and 24.74 J/(mol*K) (2100 K). This decrease is unexpected, but in agreement with [53]. These values are higher than those depicted in Figure 3, which were taken from [53], where a calculation routine is described as method of determination, which is in clear contrast to the measured data given by Vargaftik.

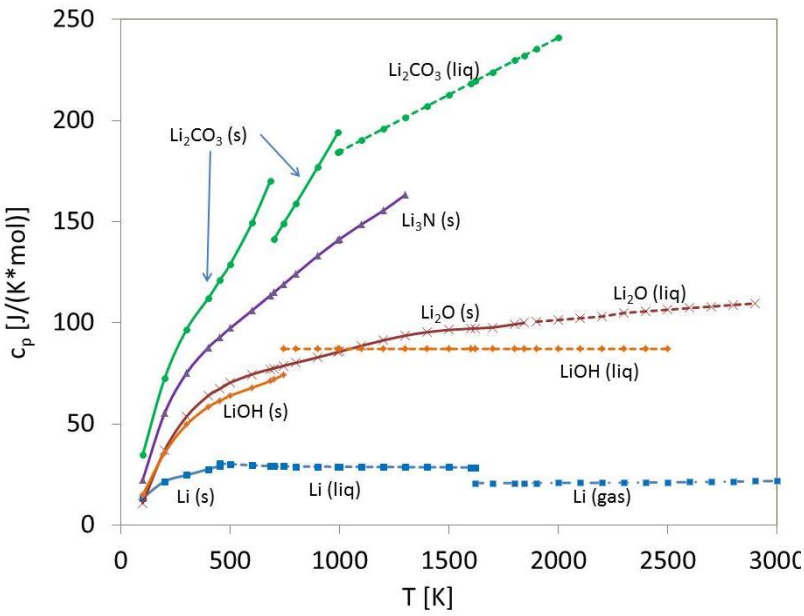

Figure 3: Specific heat capacity of possible reaction products of Lithium [54,60,70,76,77]

For Li_2CO_3, Janz et al. measured heat capacities in the temperature range from 563 K and 1173 K, which were extrapolated to low temperature data provided by Brown and Latimer [60,78]. The heat capacity of Li_2CO_3 is the highest of all compounds considered here, raising to 194 J/(mol*K) at 993 K. Janz et al. measured c_p up to a temperature of 1150 K, all higher values are based on extrapolation [53,60].

For Li_2O, the heat capacity was measured up to 1133 K by Shomate et al. and Rodigina et al. [70,77]. Higher values were extrapolated graphically [53]. Rodigina mentions an uncertainty of ±3% of the measured heat capacity.

The heat capacity of Li_3N was measured by Osborne and Flotow [76] up to 773 K, again extrapolation was necessary to extend the data up to the melting point. In general, the molar heat capacity increases with increasing molar mass of the lithium compound, as is shown in Figure 3.

2.2.3 Adiabatic flame temperature and chemical equilibrium

There is few literature stating the adiabatic flame temperatures of the reactions 1 to 6 (Table 1). Therefore, the adiabatic flame temperature for the reactions of lithium with CO_2, O_2, N_2 and H_2O was calculated using the CEA code [79] for varying stoichiometry (Figure 4). Although the heat of reaction is quite high for most of the promising reactions, which results in high adiabatic flame temperatures, the decomposition, melting or boiling of the reaction products at temperatures lower than the (theoretically calculated) adiabatic flame temperature will limit the flame temperature, which is typical for metal combustion [80]. Thermodynamic calculations and experimental work have been carried out for Lithium reacting with CO_2 by Yuasa and Isoda [81]. They calculated the adiabatic flame temperature for the reactions 2-4 from Table 1 (Li+CO_2), where the melting point of Li_2O

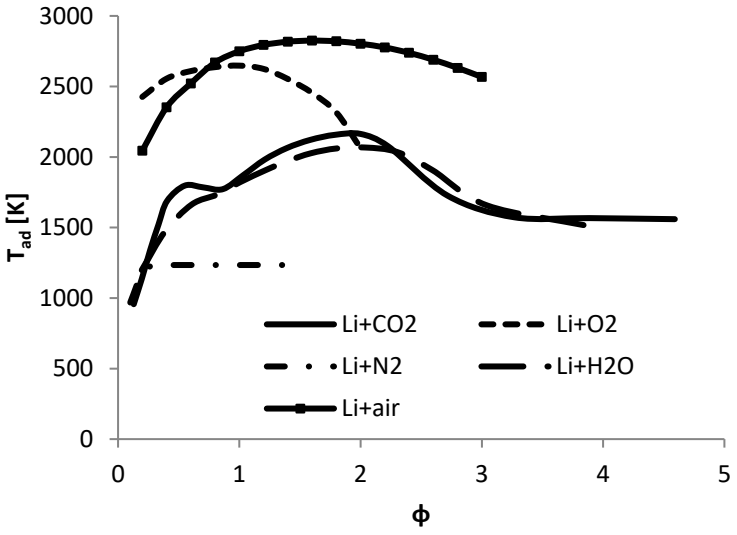

Figure 4: Adiabatic flame temperatures for lithium and the four gaseous species of interest. $\varphi = (m_{fuel}/m_{oxidizer})/(m_{fuel}/m_{oxidizer})_{stoich}$ was calculated with stoichiometric conditions from rxn 1 (N_2), rxn 2 (CO_2), rxn 5 (H_2O) and rxn 6 (O_2).

(using the value from van Arkel, [64]) or the evaporation of Lithium limited the adiabatic flame temperature, which is higher than the decomposition start temperature of Li_2CO_3. As Figure 4 shows, different reactions show temperature plateaus. The reaction of lithium with CO_2 ($\varphi = 1$ for 2 Li+2 CO_2 → Li_2CO_3+CO) shows a slight temperature dip for small CO_2 excess, in N_2 a temperature limit for large φ is visible, only air, O_2 and H_2O show

continuous trends. To get a deeper insight in prevailing phenomena, the chemical composition for the temperature calculations is presented in Figure 5. In CO_2, the decomposition of carbonate is responsible for the temperature plateau between $\varphi = 0.5$ and $\varphi = 0.8$. With increasing fuel excess, the adiabatic flame temperature is reduced and crystalline Li_2O is formed beneath gaseous lithium. The reaction with water vapour shows similar phenomena. The formation of liquid LiOH is only possible for a large H_2O excess, for higher φ, gaseous LiOH is formed, but replaced by Li_2O formation at highest φ, where the lithium excess leads to significant formation of crystalline Li_2O and gaseous lithium. The reaction $Li+O_2$ shows the highest adiabatic flame temperature, which leads to the formation of significant amounts of gaseous Li_2O. Increasing φ leads to a peak in the content of gaseous Li_2O followed by a phase change to the liquid state. Gaseous lithium becomes predominant with decreasing availability of oxygen. The nitridation reaction is rather limited in temperature; the CEA database uses a decomposition temperature of 1234 K here. With decreasing availability of N_2, the formation of liquid lithium increases. The reaction of lithium with air was calculated using N_2 as inert diluent as the adiabatic flame temperature of the oxidation reaction is significantly higher than the decomposition temperature of Li_3N and as the results of experiments with lithium particles burning in CO_2/N_2 mixtures have shown that in the presence of significant amounts of C/O compounds no nitridation products were found [82,83]. Indeed, the reaction with air shows dominant formation of Li_2O compounds with adiabatic flame temperatures comparable to those in pure O_2, which again demonstrates that decomposition effects contribute significantly when temperature calculations are carried out.

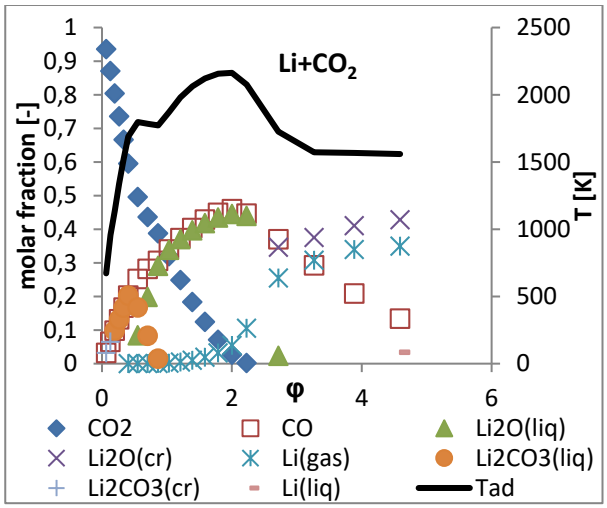

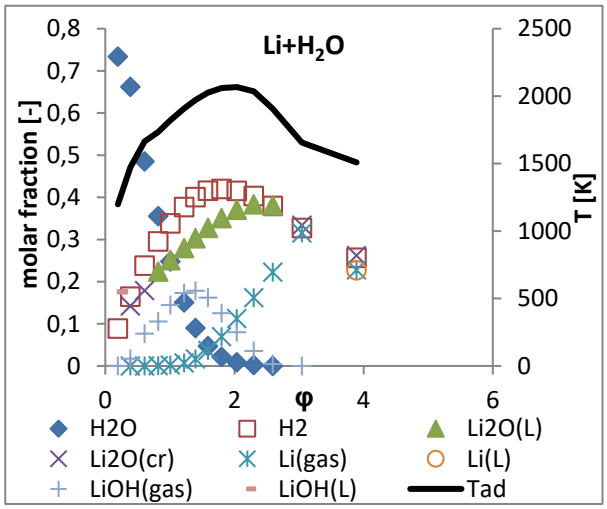

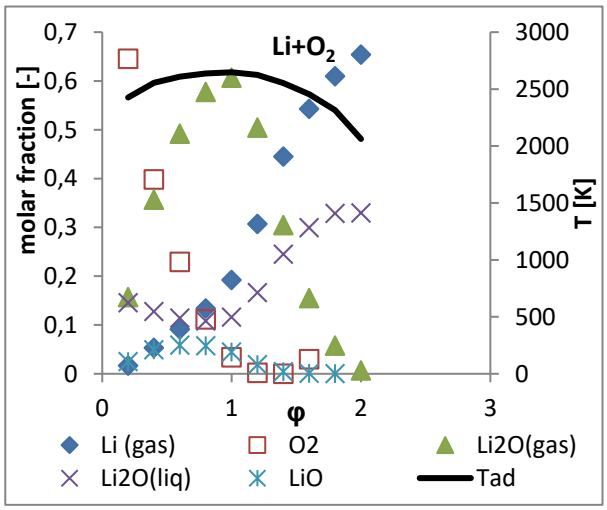

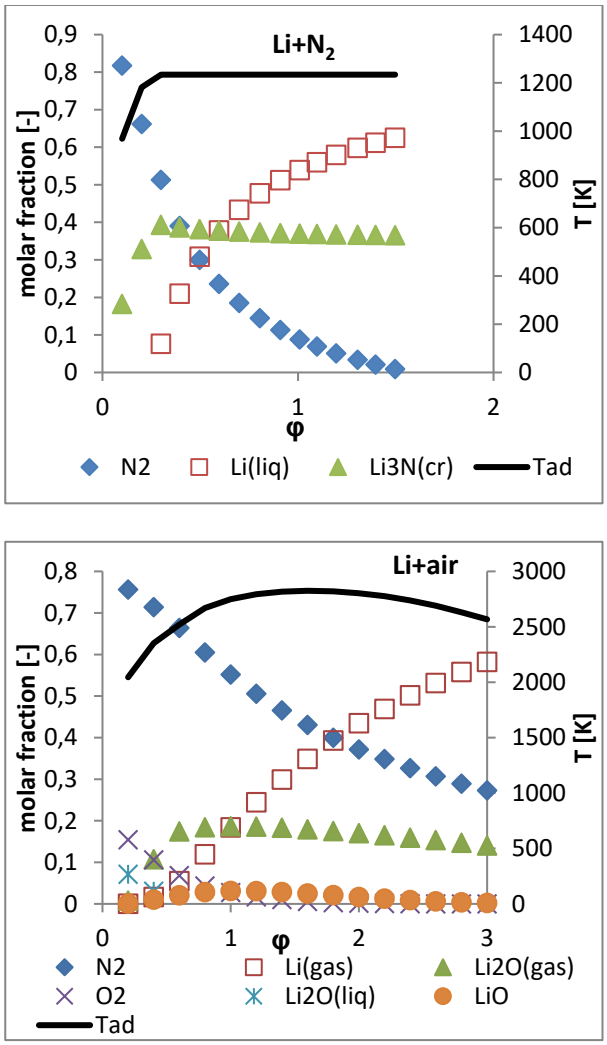

Figure 5: Chemical equilibrium composition and adiabatic flame temperature plotted against equivalence ratio. According to Table 1 molar stoichiometry was chosen as $2Li/2CO_2$ (rxn 2), $2Li/2H_2O$ (rxn 5), $4Li/O_2$ (rxn 6) and $6Li/N_2$ (rxn 1). Crystalline (cr), liquid (liq) and gaseous (gas) species were considered and are plotted when present in a mole fraction larger 0.02 (0.05 in the case of CO_2).

2.2.4 Thermal conductivity

When the Biot-number of a sample s ($Bi = \alpha L \lambda_s^{-1}$, with the heat transfer coefficient α, the characteristic length L and the thermal conductivity λ_s) is larger than unity, internal heat transfer in the material has to be considered. Furthermore, all reaction products listed in Table 1 appear in liquid or solid state in the temperature range relevant for thermal power plant processes. Thus, thermal conductivity becomes relevant when larger particles and/or layers of liquid or solid lithium compounds have to be considered. Additionally, the thermal conductivity of lithium vapour forming boundary layers above burning surfaces has to be taken into account when the heat flux from the flame to the surface of liquid lithium has to be calculated.

As Lithium melts at 453 K, its thermal conductivity is of interest for the liquid and gaseous state. In the liquid state, Davison [84] compares the thermal conductivity measurements presented by Webber, Cooke and Nikolskii. As summary and approximation of the experimental data, Davison presents the equation

$$\lambda = 21.874 + 0.056255T - 1.8325 \cdot 10^{-5}T^2\ [W/(m\ K)].$$ Equation 1

Considering all uncertainties mentioned by Davison, the uncertainty in the thermal conductivity of liquid lithium is in the order of 10%. Other data is tabulated by Vargaftik [75] and Ivanovskii [85], but no uncertainties are discussed. The data sets of Davison and Vargaftik show only minor deviations (Figure 6), but the thermal conductivity published by Ivanovskii is more than 10% lower at 1500 K, but shows a steeper, almost linear increase at higher temperature.

For gaseous lithium in the temperature range between the melting point and 2000 K, Bouledroua calculated the thermal conductivity from scattering cross sections, yielding $\lambda = 0.1049 \cdot \frac{T^{0.901}}{K}[mW/(m\ K)]$ [86]. Vargaftik presents data for the gaseous state (at saturation pressure) as well [87], but as Figure 6 shows, the difference between both data sets is quite large. Better agreement is found between Bouledroua and the work of Vargaftik published in 1991 [88], but it has to be mentioned that the measurements were carried out at pressures up to 8*10^4 Pa only. Nevertheless this work is also cited as reliable within an uncertainty range of ±5% [89,90] when compared with the thermal conductivity based on the calculation from collision integrals.

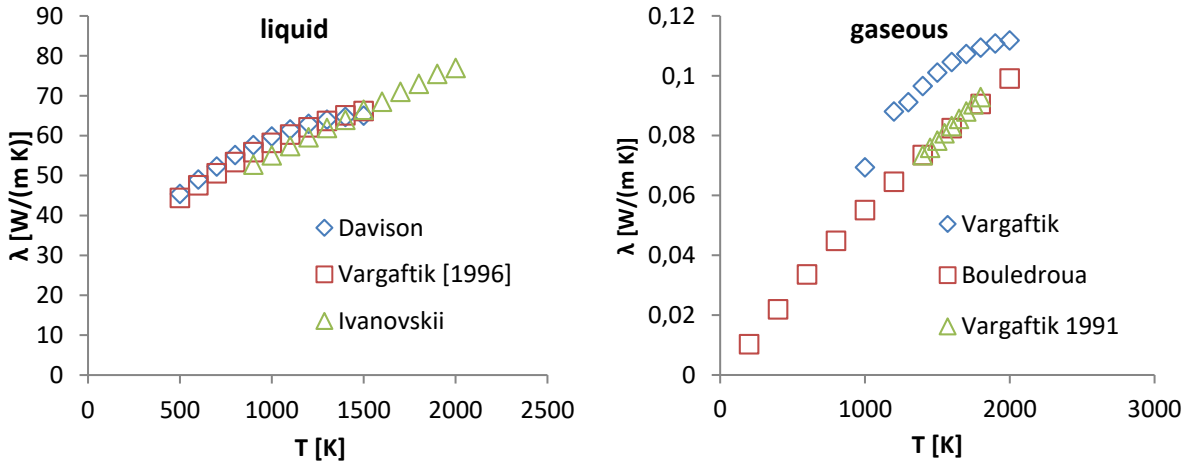

Figure 6: Thermal conductivity of liquid (left) and gaseous lithium (right).

The thermal conductivity of solid Li_2O was calculated by use of molecular dynamics by Lu et al. [91] including the influence of the lithium isotopes ^{6}Li and ^{7}Li. They report data in the temperature range from 300-1500 K for solid

Li_2O, which are depicted in Figure 7. Donato presents a fit function ($\lambda\,[Wm^{-1}K^{-1}] = 1/(0.022 + 1.784 \cdot 10^{-4}T)$) for experimental data from Ethridge [92] and Takahashi [93], this is also depicted in Figure 7. The difference between both data sets is up to a factor of 2 in the high-temperature region.

The thermal conductivity of liquid Li_2O or mixtures of lithium with Li_2O is not reported to the author's knowledge, although it would be appreciable when the combustion of larger samples is considered, or when larger amounts of liquid Li_2O have to be handled.

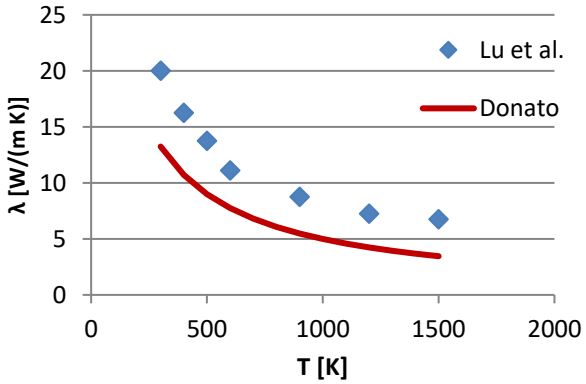

Figure 7: Thermal conductivity of solid Li_2O [91,94].

2.2.5 Vapour pressure

The vapour pressure of lithium becomes important when lithium samples are heated, and the evaporating lithium reacts exothermally in the lithium boundary region, increasing the heat flux to the lithium surface and thus increasing the evaporation rate until the boiling point is reached. As will be shown in section 2.3, in nearly all pool fires the lithium temperature stays below the boiling point, thus the vapour pressure determines the evaporation rate of lithium in these experiments. Davison [84] derives a relation ($log(P/bar) = 10.015 - 8064.5/T$) from four different sets of measured vapour pressures, stating a standard deviation of ±3.38%. In Figure 8 (note the logarithmic scale), the relation given by Davison is compared to data published by Ivanovskii et al. [85]. While at 900 K, the values from Ivanovskii are 12% larger than those published by Davison, the relation turns to the opposite above 1500 K, where the values from Davison are higher (5.6% at 1800 K).

The vapour pressure of Li_2O is low compared to that of lithium ($1.33*10^{-3}$ Pa (1273 K) [95]). Temperature dependent relations are given by Kimura et al. [96] and Kudo et al. [97]. As the low vapour pressure is confirmed

by both authors, the uncertainty (Kimuras values are one order in magnitude smaller than Kudos) is not further relevant, as in this temperature range vaporization of Li_2O is limited to a minimum (Figure 9).

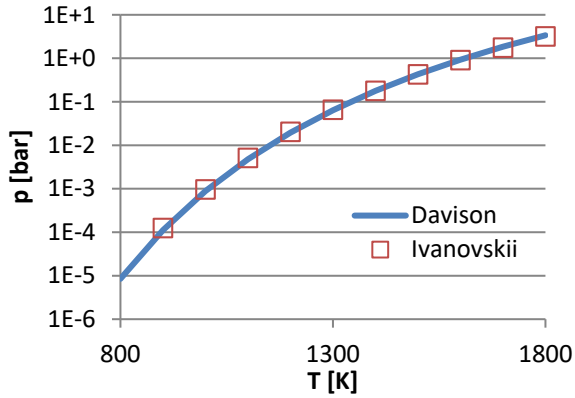

Figure 8: Vapour pressure of Li [84,85]

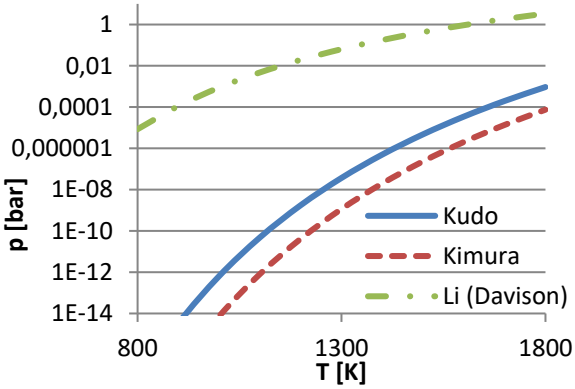

Figure 9: Vapour pressure of Li_2O [96,97]. For comparison, the vapour pressure of lithium as published by Davison is depicted [84].

As the previous sections have shown, the available data on relevant thermo-physical properties of lithium compounds, especially in the system of Li-O-C are sufficient for process design, but show non-negligible uncertainties. A summary of available data is given in Table 2. For each value, a polynomial function is given when no functional relation is presented in literature, additionally the maximum relative deviation between different literature is calculated.

Table 2: Thermo-physical properties of lithium compounds relevant for thermal processes.

	Li			
	T [K]	Polynomial	Uncertainty/Scatter	References
$c_p(T)$ [J/(mol K)]	T< 453	$5.836*10^{-7}T^3 - 5.769*10^{-4}T^2 + 0.213T - 2.669$	3.2%	[53,54,75]
	453<T<1620	$-4.501*10^{-9}T^3 + 1.22*10^{-5}T^2 - 1.093*10^{-2}T + 31.97$	4.0%	[53,54,74,75]
	1620<T	$4.584*10^{-11}T^3 + 3.928*10^{-7}T^2 – 1.825*10^{-3}T + 22.53$; [75]	[75]/[53]~2 (@1700K)	[53,75]

λ(T) [W/(Km)]	453<T<1620 liquid	$8*10^{-9}T^3 – 3*10^{-5}T^2 + 0.0591T + 22.671$	8.9%	[84,85]
	600<T<2000 gaseous	$6.690*10^{-13}T^3 - 5.455*10^{-9}T^2 + 5.796*10^{-5}T + 1.304*10^{-3}$ average from [86,88], [87] neglected as λ is 20% larger (Figure 6)	4.0% (600-2000K)	[86–88]
p_{vap} [bar]	800<T<1800	$\log_{10} p=9.942-7956.9/T$	12% (900 K) 6% (1800 K)	[84,85]
	Li_2O			
$c_p(T)$ [J/(mol K)]	300<T<1843	$3.954*10^{-8}T^3 – 1.505*10^{-4}T^2 + 0.199T + 0.867$ Extrapolated above 1050 K	3% (T<1050K)	[70,77]
	1843<T	$-3.321*10^{-9}T^3 + 2.189*10^{-5}T^2 - 3.782*10^{-2}T + 116.1$	>3%	[53,68,98]
λ(T) [W/(Km)]		$(0.0223+1.301*10^{-4}T)^{-1}$ average from [91,94]	[91]/[94]>1.4	[91,94]
p_{vap} [bar]		$10^{(13.39-22520/T)}$ [96]; $e^{(19.42-47530/T)}$ [97]	[97]/[96]~100	[96,97]
	Li_2CO_3			
$c_p(T)$ [J/(mol K)]	300<T<560	$8.929*10^{-7}T^3 – 1.155*10^{-3}T^2 + 0.651T + 19.26$	[53]/[60]=1.23 (500 K, [60] extrapol.)	[53]
	560<T<993	$1.544*10^{-8}T^3 - 1.764*10^{-5}T^2 + 0.177*T + 21.16$	[53]/[60]< 1%	[53,60]
	993<T	$-5.421*10^{-20}T^3 + 1.893*10^{-16}T^2 + 5.633*10^{-2}T + 128.3$ Extrapolated above 1150K	[53]/[60]=1.09 (1200 K)	[53,60]

2.3 Large Samples, Pool Fires and Packed Beds

A large number of past studies have investigated the combustion of large samples of lithium, the combustion over pools of liquid lithium, or within packed beds of lithium particles. In all of these different types of experiments the reaction of lithium with gaseous reaction partners is limited by oxidizer or lithium vapour transport. The definition of large samples is related to a diameter of more than 1 mm. The particle size in these experiments is definitely larger than preferred in pulverized fuel or droplet combustion, nevertheless the extent of work in this field is large compared to experiments with smaller particles and droplets suspended in gas flows, which will be discussed in section 2.4.

2.3.1 *Reaction with Water*

Lithium reacts with liquid and gaseous water, but the reaction with liquid water is less vigorous than the reactions of other alkali metals [52,99]. The reaction 2 Li + 2 H_2O → 2 LiOH + H_2 of a pea-sized piece of Lithium reacting with 250 ml water at room temperature led to a temperature increase up to 371-376 K, as shown by Markowitz [57]. No ignition of the hydrogen was observed. Also, a rate law was derived which describes the decline of the Lithium sphere's radius as $r = r_0 - kt$, with k= 36 µm/s and the initial radius r_0. In water vapour, Deal and Svec studied the reaction rate of lithium cylinders in a temperature range from 318 K to 348 K measuring the pressure of H_2 produced [100]. They found no ignition and slow reaction rates. This is in contrast to the explosive nature of other alkali metals including sodium and potassium with water [101].

Ignition of Lithium with water is possible, for example when the metal is heated to 521 K and exposed to a water spray [102], or when the material is finely divided [2,7,57,103]. Furthermore it was found, that larger lithium pieces reacting with steam formed a solid LiOH layer, which was first protective, but cracked with proceeding reaction. Through the opened pores, liquid lithium effused and showed ignition and combustion in a brilliant flame [2].

The reaction in liquid water seems little promising for a thermal process, but hydrogen production could be an alternative route to use lithium as energy carrier material [Klanchar1997] , similar to aluminum, magnesium and other light metals [11,13,15,17]. However, the activated nature of the lithium reaction with water leads to safety issues when lithium spray or powder gets into contact when exposed to water. Potential concepts for process design have to consider this, avoiding contact of molten lithium or lithium powder with water or water vapor.

2.3.2 *Reaction with Oxygen*

At moderate temperatures, the reaction of lithium with dry oxygen is negligible [57,104–106]. Tyzack and Longton [107] as well as Markowitz [104] reported an ignition temperature of 903 K in pure oxygen, the latter measured for a packed bed of 100-125 mesh lithium powder. In the same work Markowitz et al. presented TGA-curves of lithium powder exposed to dry and water-enriched gases (Figure 10). They summarized, that up to 523 K lithium does not show any weight gain due to formation of oxide, which is in accordance to other authors [105,106]. Cheburkov et al. showed, that a water vapor content of 10-15 ppm is sufficient to increase the reactivity in the temperature range from 483-913 K significantly [105]. They reported that the activation energy for the oxidation reaction of several grams of liquid Lithium is 65.3 kJ/mol for the initial reaction. A logarithmic trend was found $\left(\Delta m = k_{log}\, ln(\tau - \tau_0)\right)$ for this part of the reaction, while later on the rate became

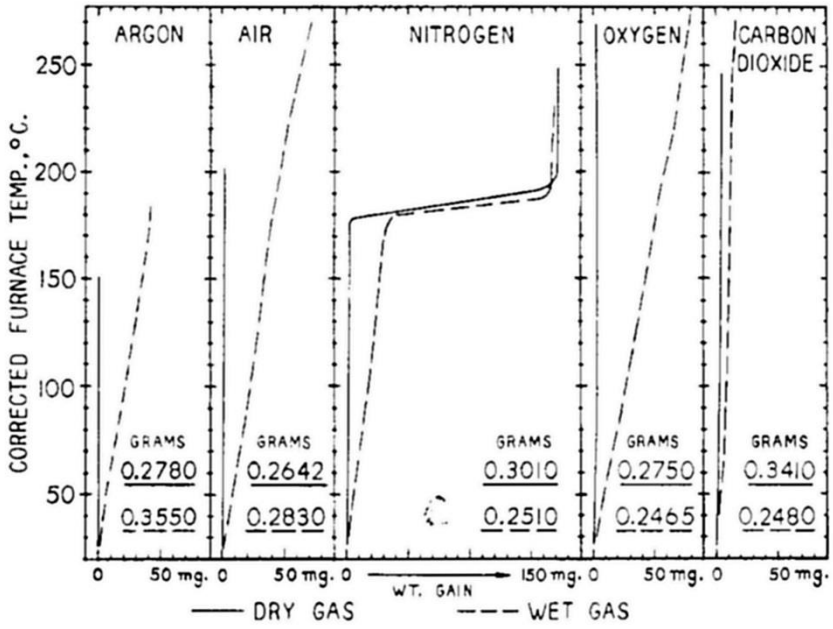

Figure 10: Weight gain of Lithium in dry and wet gases as measured by Markowitz et al. [104].

linear $\left(\Delta m = k_{lin}\,(\tau - \tau_0)\right)$, with slightly lower activation energy. The decrease in reactivity was caused by oxygen transport through the porous layer of reacted material, which had formed on the sample.

Irvine et al. investigated the reaction with oxygen at temperatures around 313K [106]. They also reported the formation of a protective layer consisting of reaction products (LiOH and $LiOH{\cdot}H_2O$) on samples cut to circular discs before reacting with moisturized oxygen.

2.3.3 *Reaction with Nitrogen*

The reaction $6\,Li + N_2 \rightarrow 2\,Li_3N$ has been studied for solid [104,108,109] and liquid lithium [7,104,109–113]. Different ignition temperatures have been reported from 443 K [104] to 873 K [114]. Here it has to be mentioned, that ignition phenomena are always related to the characteristic dimension (e.g. particle size, gas and sample temperature, and cloud number density) of an experiment. The effect of particle size, heating rate, and number density of particles has been investigated for metal particles and other fuels [19,20,115–120]. This knowledge already shows, that the ignition temperature ranges presented in the following are pointing into the direction of the temperature range in which ignition will occur for smaller particles, but requires further investigation when smaller particles are of interest.

The TGA measurements provided by Markowitz show a rapid increase in the sample mass at 443 K (Figure 3), which is attributed to the exothermic nitridation reaction. However, Rhein measured ignition temperatures between 661 K and 683 K [108]. Furthermore, Cheburkov performed measurements in dry N_2 at temperatures

between 568 K to 683 K, in which nitridation was observed [112]. The highest ignition temperature was reported by Menzenhauer, who measured ignition temperatures up to 873 K [114].

The activation energies calculated from the different experiments vary by a factor of three. In [109], nitridation of liquid lithium in an unstirred pool was investigated in a temperature range from the melting point up to 638 K, at nitrogen pressures from 10 to 50 mmHg. The activation energy was determined to be 65.3 kJ/mol. Other values mentioned in literature are 96.3 kJ/mol for experiments performed in the temperature range 568-638 K [112], and 125.6 kJ/mol at 573-673 K [110]. Gardner et al. proposed two different values of 45.2 kJ/mol [121] and 62.2 kJ/mol between 673 and 773 K [122], measured in lithium pool combustion. The large scatter in activation energies is remarkable. A possible reason is the application of different temperatures, nitrogen pressure and sample mass, which is summarized in Table 3.

Table 3: boundary conditions for the determination of activation energies for lithium reacting with N_2.

E_a [kJ/mol]	T [K]	p [bar]	sample mass [g]	reference
45.2	723-823	0.93	15	[121]
62.2	673-773	0.8	4	[122]
65.3	453-638	0.013-0.067	-	[109]
96.3	568-638	0.000667-0.26	8-17	[112]
125.6	573-673	-	3-6	[110]

For the reaction of solid lithium (which is definitely below the temperature range of interest for energy processes), it is stated that the formation of nitride layers reduces the reaction rate, as Knudsen diffusion through the nitride pores limits the transport of N_2 to the reaction zone [105,109]. Experiments carried out with molten lithium reacting with N_2 also showed a tendency to product layer formation, which inhibited further reaction [112]. Addison et al. carried out experiments with unstirred and stirred lithium [110], the latter to prevent the formation of gas transport limiting product layers. They took lithium samples of 0.5 g and heated them in a closed reactor filled with nitrogen. They measured the pressure drop of nitrogen to determine reaction progress in terms of nitrogen absorbed by the lithium sample. The experiments were carried out using stirred and unstirred lithium samples to investigate the effect of surface layer formation. Figure 11 shows the absorption of nitrogen measured for two unstirred lithium samples. As these curves show, the uptake of nitrogen w majorly follows a w^2-t law, but is shifted to lower reaction rates with proceeding conversion. No clear answer is given to the question of the surface structure below 33% of lithium conversion before the w^2 law becomes valid, but the

formation of a porous layer is suggested. Under stirred conditions, the moved surface supports a constant reaction rate typical for a direct metal-gas contact. However, Cheburkov presented experimental results which indicated that at temperatures exceeding 573 K, the nitride layer was dissolved in the remaining lithium, which kept the reaction on a level closer to the initial reaction appearing on a clean surface.

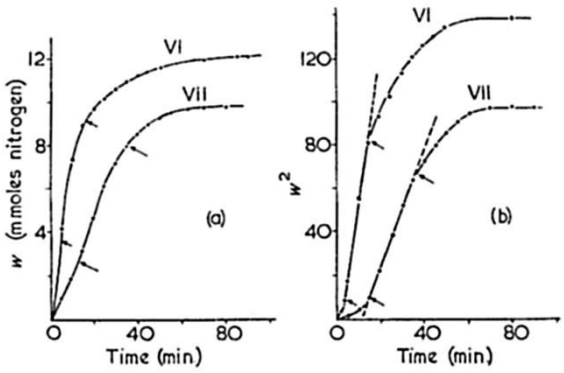

Figure 11: Nitrogen absorption rates measured at 673 K with unstirred lithium (VI: 0.5 g Li, VII: 0.41 g Li) [110].

Menzenhauer et al. studied the nitridation of lithium in pool-fires [114]. They measured a reaction rate of $\dot{m}'' = 28\ kg/(h * m^2)$ with severe aerosol formation, which accounted for 12% of the initial sample mass.

Severe influence of impurities (nitrogen contaminated with water vapor, lithium containing traces of LiOH or Li_3N) was reported. As for the oxidation reaction, the supportive influence of humidity was reported, e.g. by Markowitz ([104], see Figure 10). Barnett and co-workers found, that the nitridation reaction was catalyzed by water vapor [2]. Figure 12 depicts the ratio of the measured reaction rates of lithium with nitrogen under dry conditions and in the presence of different steam concentrations, the exponential curve fit marks the general trend to lower catalytic influence of water vapor with increasing temperature. Furthermore it is reported that the presence of water vapor did not lead to an enhanced formation of LiOH, but still the solid product found was Li_3N. Like Menzenhauer, Barnett mentioned a severe formation of aerosols during the experiments.

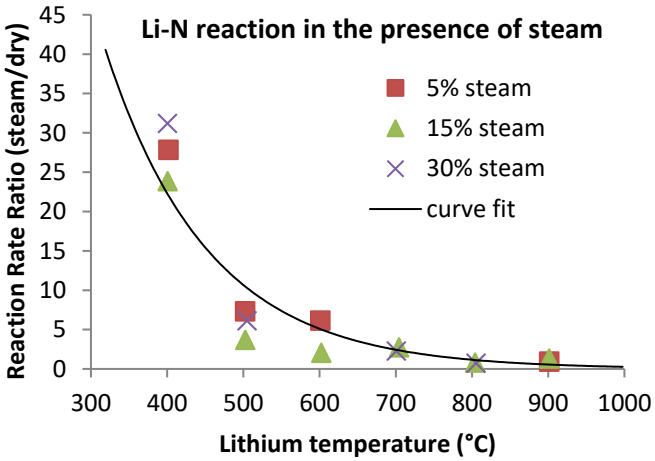

Figure 12: Reaction rate ratio of lithium with nitrogen in presence of steam and under dry conditions [2].

2.3.4 *Reaction with carbon dioxide*

Markowitz also investigated the reaction of lithium with CO_2, again dry and wet gas was used in different TGA experiments. Similar to N_2, no reaction was measured in dry CO_2, but the addition of vapour led to immediate increase in the sample mass, indicating a reaction of the lithium ([104], Figure 10). From the TGA experiments, the increase of the sample mass *w* was measured to be $w = -12.419 + 10.176 \log(t)$ [52], with w in milligrams and t in minutes. Rhein carried out measurements of lithium powder in packed beds. He found an ignition temperature of 603 K in CO_2 [7,108], with a vigorous reaction taking place in the vapour phase [111]. Yuasa et al. reported similar results [81]. In their pool fire experiments, lithium heated under inert conditions emitted reddish vapour at temperatures around 673 K, far below the boiling point. Adding CO_2, the vapour formation stopped, as the sample was coated with a greyish coating. With increasing temperature, this coating increasingly cracked, which led to a sudden increase in sample temperature and reaction rate around 1163 K. At this point, they reported a yellow-reddish flame above the sample surface, accompanied by aerosol production. In their work the color of the flame is not explained, but red is the typical wave length of gaseous elemental lithium (λ= 670 nm) and yellow may have been thermal radiation. The findings of Brockhinke et al. point out similar phenomena [46]. They describe the ignition of approx. 1 g of preheated lithium by an electric spark. During the combustion, a grey-black block was formed on the surface of the sample (Figure 13). The reaction was calm compared to that measured in air. The reaction product was identified to be Li_2O and LiC with Li_2CO_3 as by-product.

Figure 13: Black coral of reaction products on Lithium reacted with CO_2 [46].

2.3.5 *Reaction with Gas Mixtures*

In this section, the results of experiments with lithium pieces, pools or packed beds and gas mixtures are summarized, where each component should be available in the mixture in countable amounts, for example a few percent. Most of the work considered again deals with fire hazards caused by lithium, therefore lots of experiments with air-like nitrogen-oxygen mixtures were carried out.

The ignition temperature in air is reported between 589 K and 666 K [7,123,124]. Jeppson reported that small amounts of water vapour (8 mg_{H2O}/g_{air}) did not cause ignition of a lithium pool at 521 K, but the exposure of the lithium pool to a water spray caused ignition even at lower temperatures [102]. At 812 K, ignition in moist air (25 mg_{H2O}/g_{air}) was spontaneous.

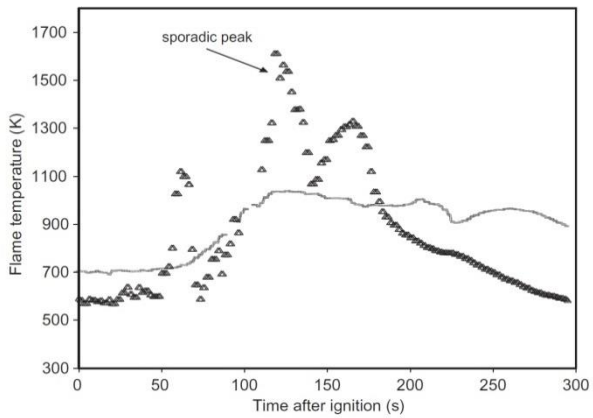

Figure 14: Temperature measured in (line) and above (triangles) lithium burning in air, 2.5 mm above the surface [125].

As a third component, CO_2 was added to N_2/Ar mixtures by Rhein to investigate the utilization of lithium powder (tested in packed-bed configuration) as propellant in the atmosphere of Venus and Mars [7,124]. The N_2/CO_2/Ar mixtures consisted of 86.6/11.2/2.2 $\%_{mol}$ and 9.2/86.7/4.1 $\%_{mol}$. The ignition temperature range was found to be 659-716 K and 583-687 K, respectively.

The measurements of both the lithium and flame temperature were carried out in numerous experiments with wide spread results. Rodgers found a maximum flame temperature of 1044 K 2.5 cm above the surface of the lithium pool [123]. Leeper, carrying out experiments to prove his technique of metal fire extinguishing [126], measured 1623 K as highest temperature. Jeppson measured two different flame temperatures (in detail described as atmosphere temperature above the lithium pool): 1423 K for lithium heated to 521 K and ignited with water spray, while it was 1163 K for lithium heated to 812 K in moist air. The lithium pool temperature was measured as 1333 and 1373 K [102]. Subramani et al. measured the time dependent temperature of 4 g lithium, which were exposed to an air flow at an initial temperature of 673 K [125]. The ignition process of the sample was delayed, a stable reaction with remarkable temperature rise appeared after 30-45 s. With proceeding time, the pool temperature rose up to 1000 K, while several bursts in the flame temperature occurred, resulting in a maximum flame temperature of 1700 K (Figure 14). Further temperature measurements were carried out by Brockhinke et al. [46], who measured the thermal radiation emitted by burning lithium with a spectroscopic technique. They compared the spectrum to a black body curve and estimated a flame temperature of 2260 K (Figure 15).

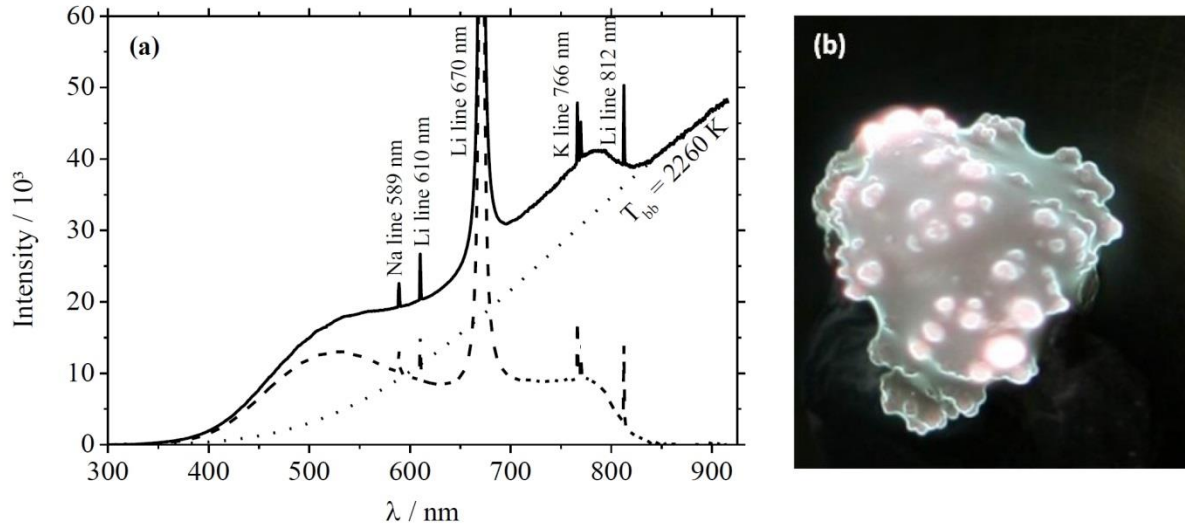

Figure 15: Spectral emission of lithium burning in air (a) and glowing lithium (product) surface (b) [46]**. The dotted line represents the best-fit black-body (thermal intensity), the dashed line is the spectrum after subtracting thermal radiation.**

Typical for the combustion of lithium in air is the formation of a solid crust, hindering the combustion process [7,46,124,125]. Subramani describes the combustion initially to take place in the pores, where gaseous lithium reacts with air, until the vaporization rate of lithium becomes large enough for the reaction front to break through the pores, which leads to the burst-like combustion events related to the temperature jumps shown in Figure 14. An example of the partial reaction at or in the surface layer is given in Figure 15b. From a similar sample, the reaction residues were investigated for their composition. In the work of Brockhinke, the white coral structure formed on top of the lithium sample was analysed to be dominated by Li_2O, while a reddish black product below the surface was identified as Li_3N [46]. This is in agreement with the findings of Barnett [2,127]. Rhein however, who studied the combustion of lithium powder in N_2/Ar/CO_2 mixtures, found that an increasing amount of nitrogen led to increasing Li_3N formation, but the CO_2 content also caused the formation of Li_2C_2 beneath small amounts of Li_2CO_3.

In general agreement, the combustion in air is described to take place in the vapour phase [2,46,102,125,127]. As a consequence, all authors mention the formation of significant amounts of aerosols. Jeppson measured the amount of aerosol formation to be in the mass range of 6-9 % of the initial lithium mass [102]. The composition of the aerosols was investigated by Barnett, who identified Li_2O as the major component [2].

Reaction rate parameters in multi-component gas mixtures are scarce in literature. Relevant data is presented by Barnett [2], who mixed nitrogen with 5-20 $\%_{mol}$ of oxygen, 5-30 $\%_{mol}$ of water vapour and a combination of both to react with molten lithium in the temperature range from 673-1173 K. It was found that the presence of oxygen reduces the nitridation reaction by reacting faster with the lithium. Li_2O was found on top of the sample and in the apparatus piping, presumably being the product of aerosol formation, while Li_3N was found in deeper layers of the lithium pool. Contrarily, water vapour catalyses the nitridation reaction at the lower temperature limit, leading to higher reaction rates. For vapour contents of 5, 15 and 30 $\%_{mol}$ balanced by nitrogen, reaction rates of 0.04, 0.18 and 0.28 $g_{Li}/(min\ cm^2)$ were found. When air-like mixtures were enriched with 5 or 15 $\%_{mol}$ of water vapour, the reaction rate was higher than in the N_2/O_2 case, but slower than in the N_2/H_2O case.

2.4 Droplets and Particles

Thermal power applications require high thermal efficiency, which requires high degrees of reaction completeness and high combustion temperatures, as well as high reaction rates to achieve high power densities [34]. The energy released from the combustion of lithium in CO_2 or O_2 provides the high energies and combustion temperatures needed for such systems. In order to provide high reaction rates and conversion efficiencies, the use of small particles in the size range of 100 µm should be explored. A possible technique to use such a fuel in power plants has recently been tested by spraying liquid lithium directly into a reaction chamber [45]. This approach avoids the need to store powdered samples, as lithium is used in larger blocks and molten directly before injecting it into the reaction chamber.

To prove the temperature level and conversion rate of lithium particles (or droplets as T_{melt}= 453 K) were carried out in pure CO_2 [32], in CO_2/N_2 mixtures [83] and in exhaust gas atmospheres [16]. The combustion of a lithium spray was investigated in [45]. A first numerical model to investigate the combustion of lithium droplets in CO_2 in computational fluid dynamics simulations (CFD) was described in [128].

2.4.1 *Particles in exhaust gas atmospheres*

The combustion of lithium particles in two atmospheres consisting of $N_2/H_2O/CO_2/O_2$ (vol. concentration [%] atm 1: 75.8, 8.0, 4.0, 12.2; atm 2: 73.9, 13.0, 6.5, 6.6) at temperatures of 1200 and 1750 K respectively is described in [16]. The experiments were carried out in a laminar drop tube reactor (DTR), which provides optical access to the burning particles as the walls are made of quartz glass. Lithium particles in the size range 50-250 µm were used in the experiments in very small particle feed rates, as the combustion of single particles should take place

without particle-particle interactions. The analysis of the combustion was carried out using a high speed camera system with high spatial resolution.

In this work, the subdivision of the combustion process in two different combustion phenomena is described. After ignition, each particle showed a very bright luminous event which was definitely larger than the initial particle size, identified as a flame of gaseous products burning at a certain stand-off distance from the particle. With proceeding burn-off, the combustion events became smaller and less luminous, pointing into the direction of surface-related combustion. Thus the typical effect of gas phase combustion with aerosol formation was confirmed, which is known from larger samples, but also the subsequent reaction at the sample surface showed that small particles do not evaporate completely before combustion. This work neither presents particle temperatures nor particle chemical compositions.

2.4.2 *Particles in CO_2*

In [32], Fischer et al. used the same camera system as already described in [16], but equipped it with new colour filters which enabled for a more accurate ratio pyrometric determination of particle temperature. Furthermore, the experiments were carried out in pure CO_2, which was heated electrically to T~ 820 K. Particles were injected with a particle size distribution ranging from 20-250 µm, with a diameter peak at approx. 85 µm. Burning particles were not only investigated by imaging pyrometry for temperature and in-situ size measurement, but also solid samples were extracted at different residence times. From the particle samples, the chemical and elemental composition of (partially) reacted particles was determined by X-ray diffraction (XRD) and CHN-analysis.

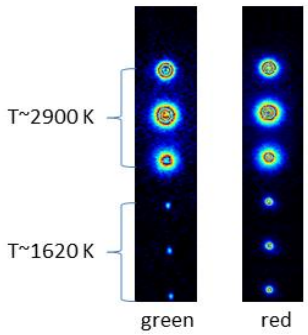

Figure 16: Sequential images of a burning particle (final diameter ~80 µm) moving downwards. Shown are false color intensities from the two channels of the ratio pyrometer. Gap between two images is 500 µs.

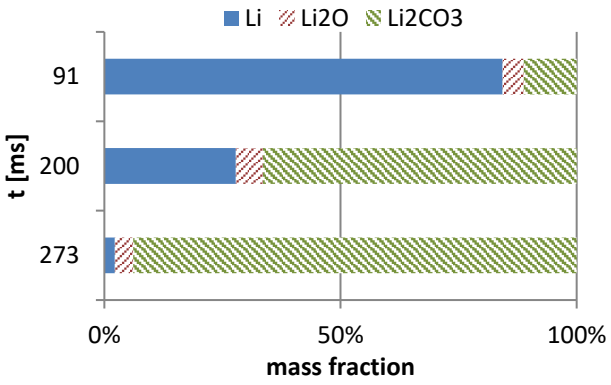

Figure 17: Mass fraction of Li, Li_2O and Li_2CO_3 from ignition (91 ms) to nearly complete burn-out.

The results presented in [32] confirm the findings from [16] regarding the first phase of particle combustion taking place in a flame layer surrounding the particle with a flame diameter approx. 5 times the diameter of the particle, followed by a second stage of combustion, which was identified as (near-) surface reaction (Figure 16). The combustion temperature of the first phase was measured in the range of 2900 K, but it is also stated that this temperature has to be handled with care, as the gas phase combustion of lithium shows several artefacts in the visual spectrum [46], which was used for pyrometry, and therefore ratio pyrometry is not a reliable method for this phase of combustion. The pyrometry measurements indicated a temperature around 1620 K for the latter stage assuming grey body radiation, which corresponds to the boiling temperature of lithium. Furthermore, equilibrium calculations also given in [32] show that this temperature still allows a significant amount of Li_2CO_3 to be formed. The results from solid sampling support this, as the sampled particles consisted of nearly pure Li_2CO_3 after 270 ms (Figure 17). The small amounts of Li_2O in the samples indicate that the formation of lithium carbonate includes the previous formation of lithium oxide. However, as the concentration of lithium oxide remained low at all sampling points, fast conversion of the oxide, formed in rxn. 3 (Table 1), in the reaction $Li_2O+CO_2 \rightarrow Li_2CO_3$ was assumed. The temperature data were used to derive apparent kinetics parameters for the global reaction $2Li+2CO_2 \rightarrow Li_2CO_3+CO$, in average a reaction rate $\dot{n}'' = 3.23 \cdot 10^{-3} exp(-40980/(RT)) p_{CO_2,s}$ [mol/(m²s)] was found to fit the measured particle temperatures. It has to be noted, that this reaction rate equation does not represent the pure chemical kinetics of the given reaction, but also includes potential transport phenomena. Especially the formation of a porous layer of reaction products on the particle surface was discussed, which would lead to pore diffusion limitation and thus require something like a shrinking reacting core model, which requires knowledge on the porous structure of the particle. The authors discuss their results as the first kinetics rate parameters to be published for sub-mm lithium particles burning in CO_2. Although the uncertainty in the chemical composition determined in these measurements is in the range of 10-15% for each component, the results give a good estimation of burning times of lithium particles in pure CO_2.

The experimentally observed changes from gas phase to surface combustion summarized above and in Figure 18 are consistent with a transition in the burning mode from the diffusion to (apparent) kinetic limits. This phenomenon is also known for the combustion of aluminium particles [129–131] and other heterogeneous combustion processes [132]. It should be noted that the kinetic and diffusion regimes are asymptotic limits, with the reaction likely occurring in a transition regime [115] for intermediate particle sizes, oxidizer concentrations and initial temperatures. For the lithium particles burning with a detached vapour-phase flame in the diffusion

limit, the evaporation rate of lithium is high enough to keep the flame layer in a certain distance from the particle surface. Under these conditions the combustion is limited by the diffusion of CO_2 from the gas phase to the flame layer. In [32] it is hypothesized that deposition of Li_2O on the particle surface leads to the formation of a layer of reaction products limiting the diffusion rate of lithium vapour, as the temperature in this regime is too high to form Li_2CO_3. Deposition of Li2O on the particle surface is assumed to be responsible for the decrease in lithium evaporation rate, which finally causes the draw-back of the reaction front on the particle surface.

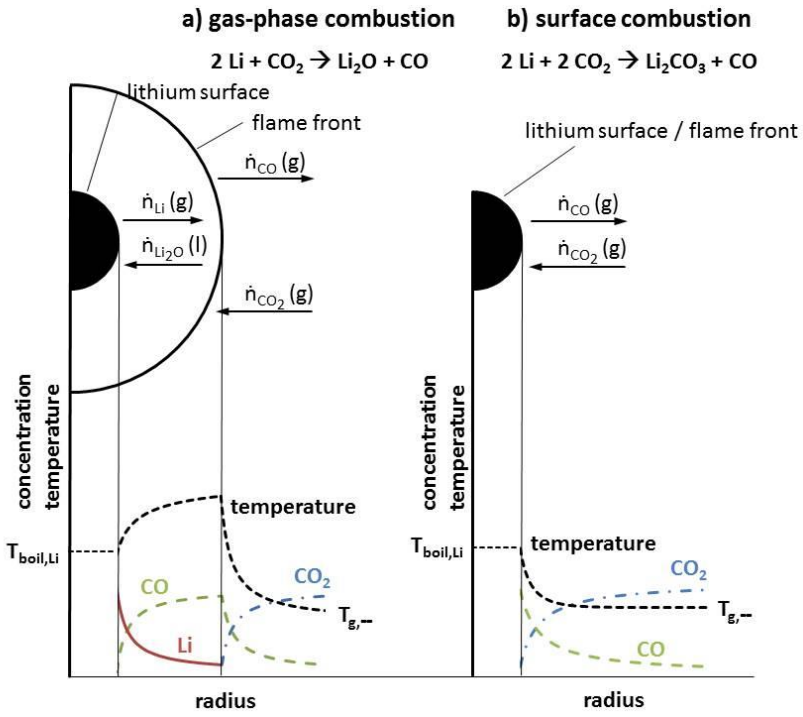

Figure 18: The two combustion regimes found for lithium particles reacting in CO2 [32,128]**. During the gas phase combustion solely formation of Li_2O (rxn. 3, reaction temperature above particle temperature) is assumed, while the reduced reaction rate during surface combustion enables to produce Li_2CO_3 by rxn. 2.**

Modelling

The experimental results described in the previous section were used to derive a model of lithium droplet combustion in CO_2. This model was implemented into a CFD-solver (Ansys Fluent) and validated against the experimental results [128]. The model is based on the following assumptions supported by the findings in [32], which have been discussed in the previous section in deeper detail:

- Lithium particles are ignited homogeneously, with lithium vapour burning in a certain stand-off distance from the particle surface. Only Li_2O is formed in this short phase (few ms) due to the expected high flame temperature.
- The inwardly diffusing reaction product Li_2O forms a layer on the droplet surface, which reduces the diffusion rate of lithium vapour, leading to the observed long-term surface reaction at 1620 K. Due to analysis of particle samples, in this phase solely Li_2CO_3 is produced.

Beneath validation to the experimental findings from [32], the model was used for parameters studies on the particle emissivity (literature values in [133] bear certain uncertainties) and ignition temperature. As the modelling shows, not only the time dependent conversion of lithium in CO_2 atmospheres is simulated correctly, also the ignition temperature of 603 K [7,108] was confirmed as suitable for the simulation of the experiment.

2.4.3 *Particles in CO_2/N_2 mixtures*

Further drop tube experiments in CO_2 atmospheres diluted with N_2 were presented in [82,83] with the same experimental techniques as described in section 2.4.2. Following remarkable phenomena are reported:

- Increasing N_2 content leads a significant reduction in the number of first stage events (gas phase combustion), which completely disappear when the volumetric fraction of CO_2 is reduced to 10%.
- Dilution of CO_2 by N_2 leads to a reduced particle temperature (named second stage or near-surface combustion in the previous section) as depicted in Figure 19, which was attributed to transport limitations (diffusion of CO_2 to the particle surface is reduced when N_2-content is increased).
- A significant amount of Li_2O was found, which increased with decreasing CO_2 content. This was interpreted as the reaction $2\ Li + 1\ CO_2 \rightarrow Li_2O + CO$ being significantly faster than the reaction $Li_2O + CO_2 \rightarrow Li_2CO_3$. This meets the expectations, as the formation of Li_2O precedes the formation of Li_2CO_3 in all cases. The results presented in section 2.4.2 summed up these two reactions two one global reaction, but in principle the sequence of the given two reactions should be valid in this case as well.

Results of combined XRD and CHN analysis for particles (d_p~ 20-250 µm, section 2.4.2) are summarized in Figure 20. These data sets represent particle samples containing only small amounts of elemental lithium (11.4% for 10% CO_2, 555 ms). A clear trend is observed, showing that reduced availability of CO_2 leads to lower lithium

consumption and favoured formation of Li_2O. Furthermore N_2 acts as an inert gas as long as CO_2 in the given amount is present.

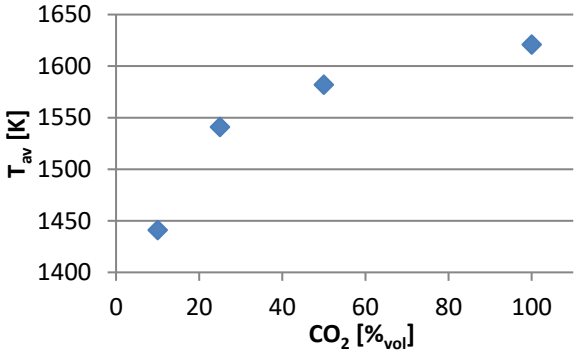

Figure 19: Average surface temperature for particles burning in CO_2-N_2 atmospheres [83].

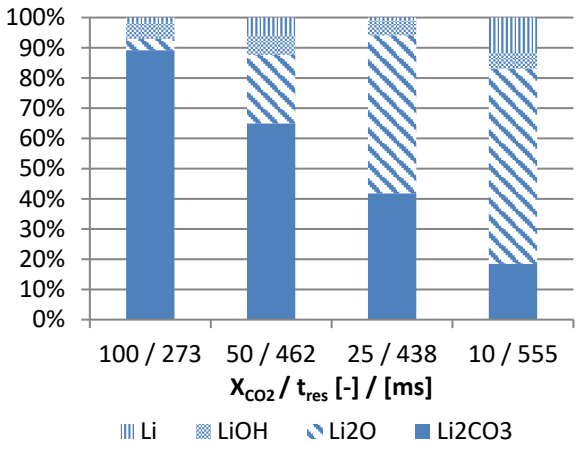

Figure 20: Composition of particle samples from drop tube experiments in atmospheres with varying composition (X_{CO2}) and residence time for final sampling position t_{res} [82,83].

2.4.4 *Spray combustion of lithium*

Kellermann et al. were the first to test lithium spray combustion in pure CO_2 [45]. They used an atomizer to produce a lithium spray. Experiments in inert atmospheres were used to measure the particle size distribution, which ranged from 50-250 µm with a clear peak at 130 µm. Subsequently, the same experiments were carried out in pure CO_2, where the lithium spray ignited when dry CO_2 was heated to 800 K before entering the reactor, or 400 K when air with "normal humidity" or a CO_2/H_2O mixture were used. The composition of the samples from dry CO_2 experiments was found to consist of Li_2CO_3 with traces of Li_2O, while the addition of water vapour led to the formation of LiOH beneath Li_2CO_3. The spray combustion of lithium was successfully demonstrated.

Spray flames have long been studied in the context of hydrocarbon combustion [134], with such flames still dominant in diesel and jet engine combustion systems [135]. In flames within dense fuel sprays, the bulk heat release from the entire fuel-air mixture yields high flame temperatures that lead to fast reaction kinetics, such that fuel-air mixing typically controls the combustion rate [134]. Similarly, in metal-fuelled combustion systems, the combustion of a cloud of metal particles will result in a high flame temperature and reduce the available oxidizer concentration through its consumption during fuel burning. This means that the reactivity of a large concentration of metal particles within a cloud cannot be predicted based on the ignition temperature or

combustion time of a single isolated particle [115]. In addition to such single-particle studies, which are important to develop models for the kinetic and diffusion rates that limit the metal-fuel consumption rate, studies are also required to understand the combustion within clouds of metal particles. Such dense metal-particle clouds would exist in any practical system that relies on a metal fuel as the main energy source, such as a lithium-fuelled power plant.

Flames can propagate through clouds of metal particles in the micron-size range [136–139]. Metal flames have been observed burning in air [137,139,140], as well as in the products of hydrocarbon flames [141–144], with such flames being observed for particles burning in both the diffusion-limited [143] as well as kinetically-limited regimes [142,143]. A detailed understanding is currently lacking for the combustion mechanism of the individual particles within such flames, and there are no quantitative models available that can predict the combustion, or flame-propagation, rate within a cloud of a certain metal at a given fuel concentration, initial temperature and initial oxidizer concentration. Recent work has suggested that the concept of laminar burning velocity may be applicable to flames through metal-particle clouds [139], but much more work needs to be done to understand the effects of flow hydrodynamics on the resulting flame speed in actual flames. Turbulent mixing has been shown to increase the flame propagation speed of metal flames significantly [139,140], but there is no available theory to predict the resulting turbulent flame speed. Our understanding of metal flames is far behind that for our more-familiar gaseous and liquid, typically hydrocarbon-based, fuels. Indeed, the authors are not aware of any studies of the combustion of burning large-concentrations of lithium powders in air, beyond the recent work of Kellermann studying a non-premixed lithium spray flame discussed above [45]. Moreover, fundamental measurements of the burning velocity, flame structure, particle-burning regimes, and oxide-product size distributions are lacking in the literature for flames through metal-particle or metal droplet clouds.

3 Conclusions

Present literature on lithium combustion was reviewed with the emphasis to provide a knowledge base regarding the energetic use of exothermal reactions of lithium with exhaust gas components for power plant processes. The literature currently available provides information on general combustion characteristics of lithium, when reacting with the most promising species CO_2 and O_2. Most of the data was produced in pool fire or other large-sample experiments. The major findings from these experiments are:

- Combustion of lithium is often accompanied by severe aerosol formation, a fact, which necessitates an elaborate flue gas treatment in a potential power plant process.
- Small amounts of water vapour catalyse the reaction of lithium with other gases.

However, power plant process require sufficiently short burning times for complete fuel conversion, leading to the concept of small particle or droplet combustion. The information available on the combustion of single droplets or particles in the sub-mm range is limited. As first results show, the combustion of such particles in gas mixtures and pure CO_2 undergoes two phases, a combustion of lithium vapour in a flame with a certain stand-off distance to the particle followed by a process taking place at the particle surface. The first process stage is accompanied by remarkable aerosol formation, which is in agreement with pool fire experiments. Furthermore, the combustion temperatures measured in pure CO_2 atmosphere are comparable to the particle temperature range known from coal combustion, which makes a thermal power plant process based on lithium possible. A first numerical model for application in CFD simulations is also available.

The literature currently available clearly shows that from the energetic point of view the combustion of lithium is a promising process, when lithium is used as storage material for renewable energy. The experimental data allow developing first models for predictive design of lithium combustion facilities. From the economical point of view, the recycling process is the key element competing with other storage techniques, and beneath the recycling quality the economic value of the combustion by-products like CO is an important factor for the practicality of the process.

It is clearly shown, that time scales and reaction products can properly be predicted, but combustion details are still missing. Apparent reaction kinetics have been derived for particles reacting in pure CO_2 but no detailed chemical kinetics is available for this step, and neither is a completely resolved model including all transport phenomena relevant in the product layer on the particle surface or the preceding gas phase combustion. First results for particle burning rates and composition of the solid lithium compounds for combustion in CO_2/N_2 mixtures are available, but the difference in the reaction scheme still needs explanation and reaction rate parameters to be described in engineering applications. Lithium particle combustion in further gases (O_2 and H_2O) and different gas mixtures needs investigation as well.

Gas phase combustion around lithium particles was noted, but a model formulation for lithium combustion in an enveloping flame around a particle is not available. This phenomenon belongs to the ignition phase, which has only been tackled rudimentary so far.

Large scale applications will require lithium spray combustion, as spraying the material directly in the reaction chamber is most favourable in terms of safety. As the conditions in dense sprays are different and transport limitations are highly expected, detailed investigations are needed to characterize this step in detail.

As many of the combustion processes are accompanied by severe aerosol formation, investigating this process is of further need, as a flue gas cleaning system has to be designed for the potential amount of aerosol to be handled.

Current work investigated the most promising reactions at atmospheric pressure or below. As closed cycles are favourable due to safety and material recovery, the question arises if pressurized lithium combustion could lead to process routes of higher efficiency.

Acknowledgement

This work was supported by the Federal Ministry of Education and Research (BMBF) under project number 03EK3007D and by the Ruhr University Research School PLUS, funded by Germany's Excellence Initiative [DFG GSC 98/3].

References

[1] D.W. Jeppson, J.L. Ballif, B.E. Chou, Lithium Literature Review : Lithiums's Properties and Interactions, Richmond, WA, 1970.

[2] D.S. Barnett, T.K. Gil, Lithium-mixed gas reactions, Fusion Technol. 15 (1989) 967.

[3] F.A. Anderson, A primer for the safe use of liquid alkali metals, Oak Ridge, Tennessee, USA, 1967.

[4] V.A. Maroni, R.A. Beatty, H.L. Brown, L.F. Coleman, R.M. Foose, C.C. McPheeters, et al., Analysis of the October 5, 1979 lithium spill and fire in the Lithium Processing Test Loop, Argonne, IL (United States), 1981.

[5] R.A. Rhein, C.M. Carlton, Extinction of lithium fires: Thermodynamic computations and experimental data from literature, Fire Technol. 29 (1993) 100–130.

[6] L.A. Parnell, D.L. Katz, J.T. Gilchrist, L.E. Bryant, J.P. Lucero, Radiography of Liquid Metal Fuel Combustion, in: Proc. 22nd Intern. Energy Convers. Eng. Conf., 1987: pp. 1–6.

[7] R.A. Rhein, The utilization of powdered metals as fuels in the atmospheres of Venus, Earth, and Mars, Pasadena, CA, 1967.

[8] W.C. Reynolds, Investigation of ignition temperatures of solid metals, Washington, D.C., 1959.

[9] D. Stocker, Climate change 2013: The physical science basis, Bern, 2013.

[10] T. Yabe, S. Uchida, K. Ikuta, K. Yoshida, C. Baasandash, M.S. Mohamed, et al., Demonstrated fossil-fuel-free energy cycle using magnesium and laser, Appl. Phys. Lett. 89 (2006) 1–4.

[11] H.Z. Wang, D.Y.C. Leung, M.K.H. Leung, M. Ni, A review on hydrogen production using aluminum and aluminum alloys, Renew. Sustain. Energy Rev. 13 (2009) 845–853.

[12] D. Wen, Nanofuel as a potential secondary energy carrier, Energy Environ. Sci. 3 (2010) 591.

[13] E.I. Shkolnikov, a. Z. Zhuk, M.S. Vlaskin, Aluminum as energy carrier: Feasibility analysis and current technologies overview, Renew. Sustain. Energy Rev. 15 (2011) 4611–4623.

[14] M.S. Vlaskin, E.I. Shkolnikov, a. V. Bersh, a. Z. Zhuk, a. V. Lisicyn, a. I. Sorokovikov, et al., An experimental aluminum-fueled power plant, J. Power Sources. 196 (2011) 8828–8835.

[15] Y. Yavor, S. Goroshin, J.M. Bergthorson, D.L. Frost, R. Stowe, S. Ringuette, Enhanced hydrogen generation from aluminum-water reactions, Int. J. Hydrogen Energy. 38 (2013) 14992–15002.

[16] M. Schiemann, P. Fischer, V. Scherer, G. Schmid, D. Taroata, Combustion of Lithium Particles: Optical Measurement Methodology and Initial Results, Chem. Eng. Technol. 37 (2014) 1600–1605.

[17] Y. Yavor, S. Goroshin, J.M. Bergthorson, D.L. Frost, Comparative reactivity of industrial metal powders with water for hydrogen production, Int. J. Hydrogen Energy. 40 (2015) 1026–1036.

[18] A. Steinfeld, P. Kuhn, A. Reller, R. Palumbo, J. Murray, Y. Tamaura, Solar-processed metals as clean energy carriers and water-splitters, Int. J. Hydrogen Energy. 23 (1998) 767–774.

[19] E.L. Dreizin, Metal-based reactive nanomaterials, Prog. Energy Combust. Sci. 35 (2009) 141–167.

[20] F. Maggi, S. Dossi, C. Paravan, L.T. DeLuca, M. Liljedahl, Activated aluminum powders for space propulsion, Powder Technol. 270 (2015) 46–52.

[21] E.L. Dreizin, M. Schoenitz, Correlating ignition mechanisms of aluminum-based reactive materials with thermoanalytical measurements, Prog. Energy Combust. Sci. 50 (2015) 81–105.

[22] C.K. Law, Fuel Options for Next-Generation Chemical Propulsion, AIAA J. 50 (2012) 19–36.

[23] P. Roy Choudhury, Slurry fuels, Prog. Energy Combust. Sci. 18 (1992) 409–427.

[24] D.L. Frost, F. Zhang, Slurry Detonation, in: F. Zhang (Ed.), Shock Wave Sci. Technol. Ref. Libr. Vol.4, Springer, 2009: pp. 169–216.

[25] E. Shafirovich, A. Varma, Metal-CO2 Propulsion for Mars Missions: Current Status and Opportunities, J. Propuls. Power. 24 (2008) 385–394.

[26] R. a. Yetter, G. a. Risha, S.F. Son, Metal particle combustion and nanotechnology, Proc. Combust. Inst. 32 (2009) 1819–1838.

[27] G.A. Risha, T.L. Connell, R.A. Yetter, Combustion of Frozen Nanoaluminum and Water Mixtures, J. Propuls. Power. 30 (2014) 133–142.

[28] Y. Huang, G.A. Risha, V. Yang, R.A. Yetter, Combustion of bimodal nano / micron-sized aluminum particle dust in air, in: Proc. Combust. Inst., 2007: pp. 2001–2009.

[29] M.K. King, Metal Combustion Efficiency Predictions for LowL * Rocket Motors, J. Spacecr. 22 (1985) 512–513.

[30] D. a. Rodriguez, E.L. Dreizin, E. Shafirovich, Hydrogen generation from ammonia borane and water through combustion reactions with mechanically alloyed Al·Mg powder, Combust. Flame. 162 (2015) 1498–1506.

[31] A. Kumar, N. Swamy, E. Shafirovich, Conversion of aluminum foil to powders that react and burn with water, Combust. Flame. 161 (2013) 322–331.

[32] P. Fischer, M. Schiemann, V. Scherer, P. Maas, G. Schmid, D. Taroata, Experimental characterization of the combustion of single lithium particles with CO2, Fuel. 153 (2015) 90–101.

[33] D.B. Beach, a. J. Rondinone, B.G. Sumpter, S.D. Labinov, R.K. Richards, Solid-State Combustion of Metallic Nanoparticles: New Possibilities for an Alternative Energy Carrier, J. Energy Resour. Technol. 129 (2007) 29.

[34] J.M. Bergthorson, S. Goroshin, M.J. Soo, P. Julien, J. Palecka, D.L. Frost, et al., Direct combustion of recyclable metal fuels for zero-carbon heat and power, Appl. Energy, under Revis. (n.d.).

[35] A. Ritchie, W. Howard, Recent developments and likely advances in lithium-ion batteries, J. Power Sources. 162 (2006) 809–812.

[36] F.T. Wagner, B. Lakshmanan, M.F. Mathias, Electrochemistry and the future of the automobile, J. Phys. Chem. Lett. 1 (2010) 2204–2219.

[37] A.C. Luntz, B.D. McCloskey, Nonaqueous Li–Air Batteries: A Status Report, Chem. Rev. 114 (2014) 11721–11750.

[38] J. Lu, Z.Z. Fang, H.Y. Sohn, A hybrid method for hydrogen storage and generation from water, J. Power Sources. 172 (2007) 853–858.

[39] Y. Wang, H. Li, P. He, H. Zhou, Controllable Hydrogen Generation from Water, Sustain. Chem. Green Chem. 3 (2010) 571–574.

[40] C. Li, P. Peng, D.W. Zhou, L. Wan, Research progress in LiBH4 for hydrogen storage : A review, Int. J. Hydrogen Energy. 36 (2011) 14512–14526.

[41] M. Klanchar, B.D. Wintrode, J. a. Phillips, Lithium−Water Reaction Chemistry at Elevated Temperature, Energy & Fuels. 11 (1997) 931–935.

[42] E.G. Groff, G.M. Faetht, Steady Metal Combustor as a Closed Thermal Energy Source, J. Hydronautics. 12 (1978) 63–70.

[43] T.G. Hughes, R.B. Smith, D.H. Kielyt, Stored Chemical Energy Propulsion System for Underwater Applications, J. Energy. 7 (1983) 128–133.

[44] S.-H. Chan, Multiphase turbulent liquid metal fuel combustion, Prog. Energy Combust. Sci. 19 (1993) 105–143.

[45] R. Kellermann, D. Taroata, M. Schiemann, H. Eckert, P. Fischer, V. Scherer, et al., Reaction Products in the Combustion of the High Energy Density Storage Material Lithium with Carbon Dioxide and Nitrogen, MRS Proc. 1644 (2014) mrsf13–1644–dd07–02.

[46] A. Brockhinke, J. Koppmann, R. Brockhinke, R. Kellermann, H. Eckert, D. Taroata, et al., Spectroscopic characterization of lithium combustion, MRS Proc. 1644 (2014) mrsf13–1644–dd08–09.

[47] B. Metz, O. Davidson, H.C. de Coninck, M. Loos, L.A. Meyer, IPCC special report on carbon dioxide capture and storage, Cambridge University Press, Cambridge, United Kingdom and New York, 2005.

[48] Y. Dessureault, P. Live, N. Skiadas, G.H.K. Pearse, E.C. Limited, A. Lamontagne, et al., NI 43-101 Technical Report Preliminary Economic Assessment of the Whabouchi Lithium Deposit and Hydromet Plant, 2012.

[49] D.R. Sadoway, Toward new technologies for the production of lithium, JOM. 50 (1998) 24–26.

[50] D.H. Deyoung, Production of lithium by direct electrolysis of lithium carbonate, US patent 4988417, 1991.

[51] J.-M. Verdier, S. Jacubert, J. Grosbois, J.-Y. Dumousseau, Continuous electrolysis of lithium chloride into lithium metal, US patent 4617098, 1986.

[52] R.A. Rhein, Lithium Combustion : A Review, China Lake, CA, 1990.

[53] M.W. Chase, NIST-JANAF Themochemical Tables, Fourth Edition, J. Phys. Chem. Ref. Data, Monogr. 9. (1997) 1–1159.

[54] T.B. Douglas, L.F. Epstein, J.L. Dever, W.H. Howland, Lithium: Heat Content from 0 to 900°, Triple Point and Heat of Fusion, and Thermodynamic Properties of the Solid and Liquid 1, J. Am. Chem. Soc. 77 (1955) 2144–2150.

[55] R. Weast, M. Astle, W. Beyer, CRC handbook of chemistry and physics, 71st ed., CRC Press, Boca Raton, Fl., 1988.

[56] R.N. Lyon, D.L.V. Katz, Liquid Metals Handbook, United States. Office of Naval Research. Committee on the Basic Properties of Liquid Metals, U.S. Atomic Energy Commission, United States, 1954.

[57] M.M. Markowitz, Alkali metal-water reactions, J. Chem. Educ. 40 (1963) 633–636.

[58] Y.I. Ostroushko, G.A. Kovda, P.I. Buchikhin, S.A. Shelkova, V.V. Alekseeva, P.N. Alekseeva, et al., Lithium, its chemistry and technology, USAEC Division of Technical Information, 1962.

[59] A. Reisman, Reactions of the Group VB Pentoxides with Alkali Oxides and Carbonates. IX. A DTA Study of Alkali Metal Carbonates, J. Am. Chem. Soc. 80 (1958) 3558–3561.

[60] G.J. Janz, E. Neuenschwander, F.J. Kelly, High-temperature heat content and related properties for Li2CO3, Na2CO3, K2CO3, and the ternary eutectic mixture, Trans. Faraday Soc. 59 (1963) 841.

[61] M.G. Ktalkherman, V.A. Emelkin, B.A. Pozdnyakov, Production of lithium oxide by decompostion lithium carbonate in the flow of a heat carrier, Theor. Found. Chem. Eng. 43 (2009) 88–93.

[62] A.N. Timoshevskii, M.G. Ktalkherman, V.A. Emel'kin, B.A. Pozdnyakov, A.P. Zamyatin, High-temperature decomposition of lithium carbonate at atmospheric pressure, High Temp. 46 (2008) 414–421.

[63] L. Brewer, J. Margrave, The Vapor Pressures of Lithium and Sodium Oxides, J. Phys. Chem. 59 (1955) 421–425.

[64] A.E. Van Arkel, E.A. Flood, N.F.H. Bright, The electrical conductivity of molten oxides, Can. J. …. 31 (1953) 1009.

[65] M.S. Ortman, E.M. Larsen, Preparation, Characterization, and Melting Point of High-Purity Lithium Oxide, J. Am. Ceram. Soc. 66 (1983) 645–648.

[66] J. Berkowitz, W. a. Chupka, G.D. Blue, J.L. Margrave, Mass Spectrometric Study of the Sublimation of Lithium Oxid, J. Phys. Chem. 63 (1959) 644–648.

[67] D.L. Hildenbrand, W.F. Hall, N.D. Potter, Thermodynamics of Vaporization of Lithium Oxide, Boric Oxide, and Lithium Metaborate, J. Chem. Phys. 39 (1963) 296.

[68] D. White, K.S. Seshadri, D.F. Dever, D.E. Mann, M.J. Linevsky, Infrared Spectra and the Structures and Thermodynamics of Gaseous LiO, Li2O, and Li2O2, J. Chem. Phys. 39 (1963) 2463.

[69] R.. Yonco, E. Veleckis, V.. Maroni, Solubility of nitrogen in liquid lithium and thermal decomposition of solid Li3N, J. Nucl. Mater. 57 (1975) 317–324.

[70] C.H. Shomate, A.J. Cohen, High Temperature Heat Content and Entropy of Lithium Oxide and Lithium Hydroxide, J. Am. Chem. Soc. 77 (1955) 285–286.

[71] W. Powers, G. Blalock, Enthalpies and Specific Heats of Alkali and Alkaline Earth Hydroxides at High Temperatures, Oak Ridge, Tennessee, USA, 1954.

[72] H. Kudo, The rates of thermal decomposition of LiOH(s), LiOD(s) and LiOT(s), J. Nucl. Mater. 87 (1979) 185–188.

[73] L.. Dinh, W. McLean II, M.. Schildbach, J.. LeMay, W.. Siekhaus, M. Balooch, The nature and effects of the thermal stability of lithium hydroxide, J. Nucl. Mater. 317 (2003) 175–188.

[74] I.I. Novikov, V.A. Gruzdev, O.A. Kraev, A.A. Odintsov, V.V. Roshchupkin, Thermophysical properties of liquid alkali metals at high temperatures, High Temp. 7 (1969) 65–68.

[75] N.B. Vargaftik, Y.S. Touloukian, Handbook of Physical Properties of Liquids and Gases, begell house, New York, Wallingford (UK), 1996.

[76] D.W. Osborne, H.E. Flotow, Lithium nitride (Li3N): heat capacity from 5 to 350 K and thermochemical properties to 1086 K, J. Chem. Thermodyn. 10 (1978) 675–682.

[77] E. Rodigina, K. Gomel'skii, Enthalpy of Beryllium and Lithium Oxides at High Temperatures, Russ. J. Phys. Chem. 35 (1961) 898–901.

[78] O.L.I. Brown, W.M. Latimer, The Heat Capacity of Lithium Carbonate from 16 to 300°K. The Entropy and Heat of Solution of Lithium Carbonate at 298°K. The Entropy of Lithium Ion, J. Am. Chem. Soc. 58 (1936) 2228–2229.

[79] B.J. McBride, M.J. Zehe, S. Gordon, NASA Glenn Coefficients for Calculating Thermodynamic Properties of Individual Species, 2002.

[80] I. Glassmann, R.A. Yetter, Combustion of Nonvolatile Fuels, in: Combustion, 4th ed., Elsevier Inc., New York, 2008: pp. 495–551.

[81] S. Yuasa, H. Isoda, Ignition and combustion of metals in a carbon dioxide stream, Symp. Combust. 22 (1989) 1635–1641.

[82] P. Fischer, M. Schiemann, V. Scherer, D. Taroata, G. Schmid, Determination of reaction kinetics of combusting Lithium particles in CO2 and CO2-N2 mixtures, in: 9th U.S. Natl. Combust. Meet., 2015: pp. 1–10.

[83] P. Fischer, M. Schiemann, V. Scherer, G. Schmid, D. Taroata, Experimental study on the combustion of Lithium particles in CO2 and CO2-N2 mixtures, in: Proc. 7th Eur. Combust. Meet., 2015.

[84] H.W. Davison, Compilation of thermophysical properties of liquid lithium, Cleveland, Ohio, 1968.

[85] M.N. Ivanovskii, V.P. Sorokin, I.V. Yagodkin, The physical principles of heat pipes, Oxford University Press, 1982.

[86] M. Bouledroua, A. Dalgarno, R. Côté, Viscosity and Thermal Conductivity of Li, Na, and K Gases, Phys. Scr. 71 (2006) 519–522.

[87] N.B. Vargaftik, Y.K. Vinogradov, Y.K. Yakimovich, Experimental study of thermal conductivity in lithium in the gaseous phase at high temperatures, J. Eng. Phys. 55 (1988) 1400–1405.

[88] N.B. Vargaftik, Y.K. Vinogradov, V.I. Dolgov, V.G. Dzis, I.F. Stepanenko, Y.K. Yakimovich, et al., Viscosity and thermal conductivity of alkali metal vapors at temperatures up to 2000 K, Int. J. Thermophys. 12 (1991) 85–103.

[89] P.S. Fialho, M.L.V. Ramires, C.A. Nieto de Castro, J. Faraleira, U. Mardolcar, Thermophysical properties of alkali metal vapours part II - assessment of experimental data on thermal conductivity and viscosity, Berichte Der Bunsengesellschaft Für Phys. Chemie. 98 (1994) 92–102.

[90] P.S. Fialho, J. Fareleira, M.L.V. Ramires, C.A. Nieto de Castro, Thermophysical properties of alkali metal vapours part I - Prediction and Correlation of Transport Properties for Monatomic Systems, Berichte Der Bunsengesellschaft. 97 (1993) 1487–1492.

[91] H. Lu, S.T. Murphy, M.J.D. Rushton, D.C. Parfitt, R.W. Grimes, Thermal conductivity and the isotope effect in Li2O, Fusion Eng. Des. 87 (2012) 1834–1838.

[92] J.L. Ethridge, D.E. Baker, A.D. Miller, Effects of Fast Neutron Irradiation on Thermal Conductivity of Li2O and LiAlO2, J. Am. Ceram. Soc. 71 (1988) C294–C296.

[93] T. Takahashi, T. Kikuchi, Porosity dependence on thermal diffusivity and thermal conductivity of lithium oxide Li2O from 200 to 900°C, J. Nucl. Mater. 91 (1980) 93–102.

[94] A. Donato, A critical review of Li2O ceramic breeder material properties correlations and data, Fusion Eng. Des. 38 (1998) 369–392.

[95] J.M. Hur, S.M. Jeong, H. Lee, Molten salt vaporization during electrolytic reduction, Nucl. Eng. Technol. 42 (2010) 73–78.

[96] H. Kimura, M. Asano, K. Kubo, Thermochemical study of vaporization of Li2O(c) by a mass spectrometric Knudsen effusion method, J. Nucl. Mater. 92 (1980) 221–228.

[97] H. Kudo, C.H. Wu, H.R. Ihle, Mass-spectrometric study of the vaporization of Li2O(s) and thermochemistry of gaseous LiO, Li2O, Li3O, and Li2O2, J. Nucl. Mater. 78 (1978) 380–389.

[98] A. Buchler, J.L. Stauffer, W. Klemperer, L. Wharton, Determination of the Geometry of Lithium Oxide, Li2O(g), by Electric Deflection, J. Chem. Phys. 39 (1963) 2299–2303.

[99] P. Pascal, Noweau Traite de Chimie Minerale, Maisson et. cie., Paris, 1966.

[100] B.E. Deal, H.J. Svec, Metal--Water Reactions. II. Kinetics of the Reaction between Lithium and Water Vapor, J. Am. Chem. Soc. 75 (1953) 6173–6175.

[101] P.E. Mason, F. Uhlig, V. Van, T. Buttersack, S. Bauerecker, P. Jungwirth, Coulomb explosion during the early stages of the reaction of alkali metals with water, Nat. Chem. 7 (2015) 250–254.

[102] D.W. Jeppson, Scoping studies: behavior and control of lithium and lithium aerosols, Richland, Wa, 1982.

[103] Kirk-Othmer, Encyclopedia of Chemical Technology, 3rd ed., John Wiley and Sons, New York, 1981.

[104] M.M. Markowitz, D.A. Boryta, Lithium Metal-Gas Reactions, J. Chem. Eng. Data. 7 (1962) 586–591.

[105] J.O. Cowles, A.D. Pasternak, Lithium Properties Related to Use as a Nuclear Reactor Coolant., Livermore, CA, 1969.

[106] W.R. Irvine, J. a. Lund, The Reaction of Lithium with Water Vapor, J. Electrochem. Soc. 110 (1963) 141–144.

[107] C. Tyzack, P.B. Longton, The oxidation of Lithium, Risley, Warrington, Lancashire, UK, 1955.

[108] R.A. Rhein, The Ignition of Powdered Metals in Nitrogen and in Carbon Dioxide, Pasadena, CA, 1964.

[109] E.F. McFarlane, F.C. Tompkins, Nitridation of lithium, Trans. Faraday Soc. 58 (1962) 997–1007.

[110] C.C. Addison, B.M. Davies, Reaction of nitrogen with stirred and unstirred liquid lithium, J. Chem. Soc. A Inorganic, Phys. Theor. (1969) 1822–1827.

[111] R.A. Rhein, Preliminary experiments on ignition in carbon dioxide, Combust. Flame. 8 (1964) 346–348.

[112] V.I. Cheburkov, A.N. Rozanov, Kinetics of Reaction of Liquid Lithium with Oxygen and Nitrogen, Met. Christyky Met. 7 (1968) 168–173.

[113] I.E. Lyublinski, A. V Vertkov, V.A. Evtikhin, Application of lithium in systems of fusion reactors. 1. Physical and chemical properties of lithium, Plasma Devices Oper. 17 (2009) 42–72.

[114] P. Menzenhauer, W. Peppler, K. Sonntag, Brandverhalten von Kalium und Lithium - KfK 3313, Karlsruhe, 1982.

[115] M. Soo, S. Goroshin, J.M. Bergthorson, D.L. Frost, Reaction of a Particle Suspension in a Rapidly-Heated Oxidizing Gas, Propellants, Explos. Pyrotech. (2015) n/a–n/a.

[116] Y. Liu, M. Geier, A. Molina, C.R. Shaddix, Pulverized coal stream ignition delay under conventional and oxy-fuel combustion conditions, Int. J. Greenh. Gas Control. 5 (2011) S36–S46.

[117] M.K. King, Ignition and Combustion of Boron Particles and Clouds, AIAA J. 19 (1982) 294–306.

[118] B.T. Bojko, P.E. DesJardin, E.B. Washburn, On modeling the diffusion to kinetically controlled burning limits of micron-sized aluminum particles, Combust. Flame. 161 (2014) 3211–3221.

[119] K. Annamalai, W. Ryan, Interactive processes in gasification and combustion. Part I: Liquid drop arrays and clouds, Prog. Energy Combust. Sci. 18 (1992) 221–295.

[120] K. Annamalai, W. Ryan, S. Dhanapalan, Interactive processes in gasification and combustion—Part III: Coal/char particle arrays, streams and clouds, Prog. Energy Combust. Sci. 20 (1994) 487–618.

[121] M.P. Gardner, R.E. Altermatt, Kinetics of the reaction of hydrogen and nitrogen with molten lithium, in: Lithium Curr. Appl. Sci. Med. Technol., Charlotte, NC, 1983: pp. 195–206.

[122] M.P. Gardner, M.M. Nishina, Kinetics of the reactions of hydrogen, nitrogen, and hydrogen/nitrogen mixtures with molten lithium, J. Phys. Chem. i (1981) 2388–2392.

[123] S.J. Rodgers, W.A. Everson, Extinguishment of alkali metal fires, Fire Technol. 1 (1965) 103–111.

[124] R.A. Rhein, Ignition and Combustion of Powdered Metals in the Atmospheres of Venus, Earth, and Mars., Astronaut. Acta. 11 (1965) 322–327.

[125] A. Subramani, S. Jayanti, On the occurrence of two-stage combustion in alkali metals, Combust. Flame. 158 (2011) 1000–1007.

[126] L.J. Leeper, S.P. Park, H. Gunther, W.B. Lake, Fire Extinguishing, US 3475332, 1969.

[127] D. Barnett, M. Kazimi, The consequences of lithium fires in the presence of steam, Fusion Technol. 15:2 (1989) 839–846.

[128] P. Fischer, M. Schiemann, V. Scherer, P. Maas, D. Taroata, G. Schmid, A simple numerical model of the combustion of single Lithium particles with CO2, Fuel, Accept. Publ. (n.d.).

[129] K. Brooks, M. Beckstead, Dynamics of aluminum combustion, J. Propuls. Power. 11 (1995) 769–780.

[130] M.W. Beckstead, Y. Liang, K. V. Pudduppakkam, Numerical Simulation of Single Aluminum Particle Combustion (Review), Combust. Explos. Shock Waves. 41 (2005) 622–638.

[131] T. Bazyn, H. Krier, N. Glumac, Evidence for the transition from the diffusion-limit in aluminum particle combustion, Proc. Combust. Inst. 31 II (2007) 2021–2028.

[132] R.A. Yetter, F.L. Dryer, Metal particle Combustion and Classification, in: H.D. Ross (Ed.), Microgravity Combust. Fire Free Fall, Academic Press, New York, 2001: pp. 419–478.

[133] M. Rosenberg, R.D. Smirnov, A.Y. Pigarov, On thermal radiation from fusion related metals, Fusion Eng. Des. 84 (2009) 38–42.

[134] A.L. Sánchez, J. Urzay, A. Liñán, The role of separation of scales in the description of spray combustion, Proc. Combust. Inst. 35 (2015) 1549–1577.

[135] J.M. Bergthorson, M.J. Thomson, A review of the combustion and emissions properties of advanced biofuels and their impact on existing and future engines, Renew. Sustain. Energy Rev. 42 (2014) 1–46.

[136] H.M. Cassel, Some fundamental aspects to dust flames, 1964.

[137] S. Goroshin, I. Fomenko, J.H.S. Lee, Burning velocities in fuel-rich aluminum dust clouds, Symp. Combust. 26 (1996) 1961–1967.

[138] S. Goroshin, F.D. Tang, A.J. Higgins, J.H.S. Lee, Laminar dust flames in a reduced-gravity environment, Acta Astronaut. 68 (2011) 656–666.

[139] P. Julien, J. Vickery, S. Goroshin, D.L. Frost, J.M. Bergthorson, Freely-propagating flames in aluminum dust clouds, Combust. Flame, under Revis. (n.d.).

[140] P. Julien, J. Vickery, S. Whiteley, A. Wright, S. Goroshin, J.M. Bergthorson, et al., Effect of scale on freely propagating flames in aluminum dust clouds, J. Loss Prev. Process Ind. 36 (2015) 230–236.

[141] M. Soo, P. Julien, S. Goroshin, J.M. Bergthorson, D.L. Frost, Stabilized flames in hybrid aluminum-methane-air mixtures, Proc. Combust. Inst. 34 (2013) 2213–2220.

[142] P. Julien, M. Soo, S. Goroshin, D.L. Frost, J.M. Bergthorson, N. Glumac, et al., Combustion of Aluminum Suspensions in Hydrocarbon Flame Products, J. Propuls. Power. (2014) 1–8.

[143] P. Julien, S. Whiteley, S. Goroshin, M.J. Soo, D.L. Frost, J.M. Bergthorson, Flame structure and particle-combustion regimes in premixed methane-iron-air suspensions, Proc. Combust. Inst. (2014) 3–10.

[144] J. Palecka, P. Julien, S. Goroshin, J.M. Bergthorson, D.L. Frost, A.J. Higgins, Quenching distance of flames in hybrid methane–aluminum mixtures, Proc. Combust. Inst. 35 (2015) 2463–2470.